



TECHNISCHE
UNIVERSITÄT
WIEN

Vienna University of Technology

Diplomarbeit

Base Metal Complexes with PCP Pincer Ligands

ausgeführt zum Zwecke der Erlangung des akademischen Grades eines

Diplom-Ingenieurs

unter der Leitung von

a.o. Univ. Prof. Dipl. Ing. Dr. Karl Kirchner

Dipl. Ing. Dr. Matthias Mastalir

eingereicht an der Technischen Universität Wien

Fakultät für Technische Chemie

von

Wolfgang Eder

Matr.Nr. 0805747

Markt 61

5570 Mauterndorf

Wien, im November 2018

Wolfgang Eder

Ich habe zur Kenntnis genommen, dass ich zur Drucklegung meiner Arbeit unter der Bezeichnung

Diplomarbeit

nur mit Bewilligung der Prüfungskommission berechtigt bin.

Ich erkläre weiters Eides statt, dass ich meine Diplomarbeit nach den anerkannten Grundsätzen für wissenschaftliche Abhandlungen selbstständig ausgeführt habe und alle verwendeten Hilfsmittel, insbesondere die zugrunde gelegte Literatur, genannt habe.

Weiters erkläre ich, dass ich dieses Diplomarbeitsthema bisher weder im In- noch Ausland (einer Beurteilerin/einem Beurteiler zur Begutachtung) in irgendeiner Form als Prüfungsarbeit vorgelegt habe und dass diese Arbeit mit der vom Begutachter beurteilten Arbeit übereinstimmt.

Ort, im November 2018

Wolfgang Eder

Acknowledgements

First of all, I would like to thank Prof. Karl Kirchner for giving me the opportunity to work on my master thesis in his research group. I am grateful for the support and motivation he has given me throughout my work and for introducing me to this very interesting branch of chemistry.

I would also like to thank my friends and colleagues Matthias Mastalir, Mathias Glatz, Gerald Tomsu, Daniel Himmelbauer, Julian Brünig, Jan Pecak, Stefan Weber, Dina lebed, Markus Rotter as well as Nikolaus Gorgas of the Kirchner group, for all their support and the know-how they provided me with during my work. The countless memorable and entertaining evenings we spent together, whether at university or in certain high class first district establishments, I will always keep in fond memory.

I would also like to thank Dr. Berthold Stöger for X-ray diffraction measurements, and for the numerous interesting conversations and eventful hours.

I want to thank my girlfriend Julia for her love, support and understanding. ¡Te quiero pequeña! Thank you for your patience while proof reading and your help in finalizing this thesis.

Finally, I would like to express my deepest gratitude to my parents and family. Without their support throughout the years, this accomplishment would not have been possible. Thank you!

Abstract

Transition metal complexes have received great attention in chemistry due to their ability to catalyze a multitude of reactions. Among the myriads of ligand systems known in literature, pincer ligands, owing to their great stability and reactivity, as well as their excellent modifiability, have shown to be powerful tools in various areas in organometallic chemistry.

Pincer ligands are tridentate ligands, that feature a meridional coordination geometry. They consist of an aromatic or aliphatic backbone and two two-electron donor groups, that are connected to the backbone with different linkers such as CH₂, NH, NR, O. The oldest class of pincer ligands are PCP pincer ligands, most commonly featuring a benzene backbone and phosphines as electron donor groups. Although presently many PCP complexes with late transition metals are known, only very few such complexes, featuring early transition metals, exist in literature. This is due to the difficulty of creating the σ -carbon-metal bond, as generally only noble metals are able to activate C-H bonds. In an attempt to facilitate the formation of σ -C-M bonds, this work describes the synthesis of PCP pincer ligands bearing bromine moieties bonded on the *ipso* carbon of the benzene backbone.

The newly generated ligands were shown to effectively form PCP pincer complexes with a wide variety of base metals. Starting from the metal carbonyl complexes, chromium, molybdenum, tungsten as well as manganese, iron and cobalt PCP complexes were successfully synthesized and fully characterized. Nickel PCP complexes were obtained by directly reacting the metal with the ligand in acetonitrile. All compounds were characterized by means of NMR, HRMS and IR spectroscopy as well as single crystal X-ray diffraction.

Kurzfassung

Übergangsmetallkomplexen wurde in der Chemie viel Aufmerksamkeit geschenkt, da sie eine Vielzahl an Reaktionen katalysieren können. Unter der Vielfalt an Ligandensystemen, die in der Literatur bekannt sind, haben sich Pincer Liganden, durch ihre große Stabilität und Reaktivität, sowie ihre herausragende Modifizierbarkeit, als leistungsstarke Werkzeuge in verschiedenen Bereichen der metallorganischen Chemie etabliert.

Pincer Liganden sind Tridentate, die eine meridional Koordinationsgeometrie aufweisen. Sie bestehen aus einem aromatischen oder aliphatischen Grundgerüst, mit dem zwei zwei-Elektronendonoren durch Linker, wie etwa CH_2 , NH , NR , oder O , verbunden sind. Die älteste Klasse an Pincer Liganden sind PCP Pincer Liganden, die gemeinhin aus einem Benzolgrundgerüst bestehen und Phosphine als Elektronendonoren besitzen. Obwohl heutzutage eine Vielzahl von PCP Komplexe mit späten Übergangsmetallen bekannt sind, gibt es nur eine geringe Anzahl dieser Komplexe mit frühen Übergangsmetallen in der Literatur. Ein Grund dafür ist die Schwierigkeit der Bildung einer Kohlenstoff-Metall σ -Bindung, da generell nur Edelmetalle fähig sind C-H Bindungen zu aktivieren.

In einem Versuch die Bildungen von σ -C-M Bindungen zu erleichtern, beschreibt diese Arbeit die Synthese von PCP Pincer Liganden, die Brom-Substituenten an der *ipso*-Position des Benzolgrundgerüsts aufweisen.

Diese neu synthetisierten Liganden erwiesen sich als effektiv in der Herstellung von PCP Pincer Komplexe mit unedlen Metallen. Ausgehend von den Metall-Carbony-Komplexen wurden erfolgreich die PCP Komplexe von Chrom, Molybdän, Wolfram, Mangan, Eisen, sowie Kobalt synthetisiert und charakterisiert. Die Nickel PCP Komplexe wurden durch direkte Reaktion des Liganden mit Nickelmetall in Acetonitril hergestellt. Die Verbindungen wurden mittels NMR, HRMS und IR Spektroskopie, sowie mittels Einkristallröntgenbeugung charakterisiert.

Table of Contents

1. Introduction	2
1.1. Pincer Ligands	3
1.2. Modifiability of Pincer Ligands	4
1.3. Phosphines	6
1.4. PCP Pincer Complexes	7
1.4.1. Group 10 PCP pincer complexes	7
1.4.2. Group 9 PCP Pincer Complexes	13
1.4.3. Group 8 PCP Pincer Complexes	18
1.4.4. Group 7 PCP Pincer Complexes	23
1.4.5. Group 6 PCP Pincer Complexes	26
1.4.6. Complexation Methods for PCP Pincer Complexes	29
2. Experimental Part	34
2.1. Synthesis of the Ligand	34
2.2. Synthesis of Complexes	36
3. Results and Discussion	43
3.1. Ligand design and synthesis	43
3.2. Complex synthesis	45
4. Conclusion	59
5. References	60

1. Introduction

A very important aspect of organometallic chemistry is the synthesis of highly reactive transition metal complexes, that are able to function as catalysts in various reactions in chemical synthesis. For this purpose, in homogenous as well as heterogenous catalysis, systems based on precious metals are still widely used, as they commonly show higher reactivity and selectivity as well as stability, than systems containing base metals. However, recently, efforts were made to find highly reactive systems that utilize base metals in order to replace catalysts based on precious metals. This makes sense, as precious metals are more expensive, show higher toxicity and, in regard to the ever-important aspect of sustainability and environmental consciousness, have lower availability and concentration in ores.¹

Due to their great modifiability, pincer ligands show great promise in creating these kind of reactive base metal complexes and indeed, recently, various base-metal based catalysts bearing PNP pincer ligands were published.²⁻⁵

Despite these promising developments with PNP pincer ligands, base metal complexes with the longer known PCP pincer ligands are currently quite rare in literature and thus an interesting research topic.⁶

Reasons for the lack of base-metal PCP pincer ligands are the scarcity of suitably substituted benzene precursors that additionally often require tedious, multistep synthesis in order to modify their stereochemical properties.⁶ Furthermore the great stability of the *ipso* C-H bond in 1,3-substituted benzene derivatives, used for the synthesis of PCP ligands, hampers reaction with many non-precious metals.⁷

To enhance the acidity of the *ipso* C-H bond, the Kirchner group introduced PCP pincer ligands based on 1,3 diaminobenzene moieties. However due to the acidity of the NH-linker groups, the use of strong base was not possible and only complexes with Ni, Pd and Pt, i.e. metals that were able to directly activate the *ipso* C-H bond, were obtained.⁶ In a next step, the acidic NH linkers were replaced by NMe groups, thus allowing the use of strong base in order to facilitate carbon-metal bond formation. This allowed access to novel Ni and Co PCP pincer complexes.⁸⁻¹⁰

With the same ligand system, it was also possible to create the first tungsten hydride PCP complex via oxidative addition under solvothermal conditions.¹¹ Later, in a further attempt to increase the acidity of the *ipso* C-H bond, a new ligand system based on a pyrimidine backbone, was introduced. However, due to the directing effect of the

nitrogen moieties in the pyrimidine ring, the *ipso* carbon could not be deprotonated with *n*-BuLi and no complexes with Co were obtained. Ni complexes were created in good yields, by only using trimethylamine (TEA) as base.¹²

Using solvothermal conditions, Mo and W hydride PCP complexes were also synthesized using this ligand, showing that indeed an increase in acidity of the *ipso*-C-H bond had occurred.¹³

The present work deals with the synthesis of PCP pincer ligands based on the 1,3-dimethylbenzene scaffold. In order to activate the *ipso* carbon position even more, the *ipso* hydrogen was exchanged for a bromine substituent, with the aspiration of facile carbon metal bond creation *via* transmetalation, using ligand salts created in metal-halogen exchange reactions. Furthermore, it was anticipated that this would also allow for the formation of novel base metal PCP pincer complexes by means of oxidative addition reactions, as the bond-dissociation energy of the C-Br bond is lower than that of a C-H bond.⁷

1.1. Pincer Ligands

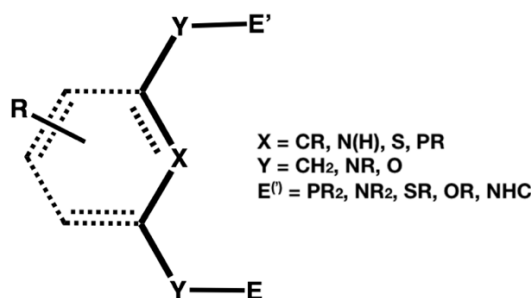


Figure 1 General structure of pincer ligands

Pincer Ligands¹⁴ are chelating, tridentate ligands based on aliphatic or aromatic frameworks. Two electron donor groups (E) are attached to the framework with linker groups. (Y). The electron donor groups usually contain NR₂, SR, OR, NHC or PR₂ moieties. The linker groups most commonly consist of nitrogen (NH, NR), carbon (CH₂) or oxygen (O) substituents. The third coordination site (X) is part of the organic backbone and forms a σ -bond to the metal center. These structural properties cause the ligand to be rigid generally enforcing a meridional coordination geometry around

the metal center. Tridentate ligands that favor a facial geometry are not termed pincer ligands. The modular structure of pincer ligands allows for fine-tuning of their electronic and steric properties without changing the coordination geometry.¹⁵ This makes them powerful tools in ligand design, providing huge variability and reactivity with great stability.

1.2. Modifiability of Pincer Ligands

One major advantage of pincer ligands is their facile modifiability. By varying the components of the ligand, the steric and electronic properties can be adjusted for each metal and synthetic problem.

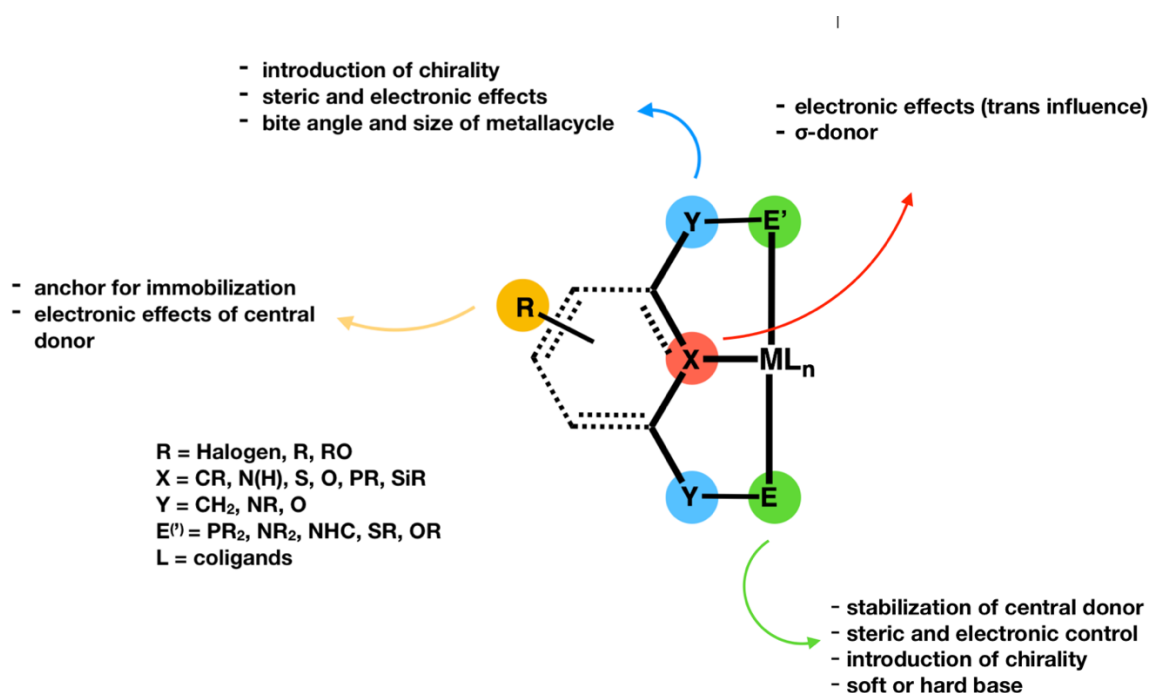


Figure 2 Control of electronic and steric properties of pincer ligands

Many pincer ligands feature aromatic scaffolds, meaning that the embedded σ -donor is of sp^2 hybridization. C and N moieties are the most common central donors in this group. However, there are also examples in literature where other central donors, such as S, O, P and Si are used.¹⁶⁻¹⁹ The variation of X can exert great electronic effects on the system as it functions as a strong donor, that shows strong trans influence.²⁰ This can make the ligands trans to the donor more labile and reactive. Another interesting aspect occurs when using aliphatic backbones. In this case the sp^3 hybridized donor can shift from the typical meridional to a facial coordination mode when

accommodating bulky co-ligands or other ligands that coordinate facially. Hence, introduction of sp^3 hybridized central donors can introduce coordination capabilities that are not conceivable with aromatic systems.^{15,21}

The other coordination centers E and E' usually consist of P, N, O, S or carbene groups. E and E' can either be of the same sort, for example two phosphine moieties, or mixed groups can be used. The nomenclature of pincers is derived from the three coordinating groups and simply states the coordinating atoms in order, e.g. PCP, PNP, PNN, or CNC.

These donor groups are crucial as they stabilize the metal center. For example, using benzene derivatives just as monodentate would prove to be difficult, as they can easily be lost *via* reductive elimination or protonation reactions. The electronic properties of the metal center can also be greatly influenced and tuned by variation of the donor or acceptor strengths of E and E'. Moreover, by using different donor atoms, one stronger binding than the other, hemilability can be observed.²² This means that the weaker bonding donor can be replaced from the metal center (for example by substrate) and re-associate immediately when needed. This behavior can increase the reactivity of catalysts when compared to other non-labile complexes.²³

By changing the bulkiness of the substituents located on E⁽ⁱ⁾ it is also possible to adjust the steric demand of the donor groups, and thus the access to the metal center, without causing much change of their electronic properties. The substituents on the electron donors can also be chiral, therefore introducing a pool of chirality into the pincer system. The linker groups Y, that bond the electron donors to the organic backbone, consist in most cases, of CH₂, NH, NMe, NEt or O moieties. Rarely other linking groups, such as S, are used.²⁴ They can, on the one hand, influence the electronic properties of the donor groups, particularly, when using phosphine moieties. On the other hand, the bulkiness of Y can also regulate the bite angle of the pincer. When using linking groups with acidic hydrogens (e.g., NH, CH₂) they can also play important roles in catalytic cycles *via in-situ* formation of unsaturated intermediates, that are then able to undergo acid-base reactions with the substrate (metal ligand cooperation, bifunctional catalysis).²⁵ It is also possible to introduce chirality into pincer ligands *via* the linking groups.²⁶

1.3. Phosphines

Phosphine moieties are widely used as donor groups in pincer ligands, as they are strong donors that allow for their steric and electronic properties to be adjusted in a methodical way. Generally, phosphines function as two electron σ donor, π -acceptor ligands. The lone pair located on the phosphorus atom is donated into an empty orbital of the metal forming a σ -bond. The σ donor strength of the phosphines can be regulated by the substituents bonded on the phosphines. Generally, electron withdrawing groups reduce, while electron donating groups enhance the σ donor strength. However, in contrast to the similar amine donors, phosphines can also function as π -acceptor ligands. This is possible as the $\sigma^*_{(P-R)}$ molecular orbitals of the phosphines are energetically lower than the corresponding $\sigma^*_{(N-R)}$ orbitals of amines and can therefore be used for π -back-bonding. The energy levels of the orbitals can also be regulated by the electronegativity of the substituents of the phosphorus. As a consequence, the σ donor/ π -acceptor strength of the phosphine donors can be tuned and regulated by the mere variation of its substituents.²⁷

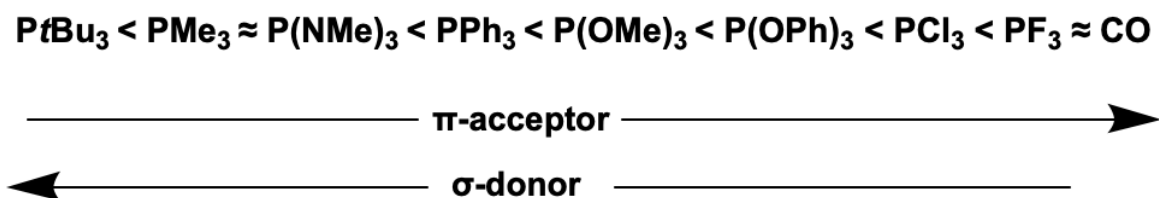


Figure 3 Electronic properties of phosphines according to Tolman²⁷

Similarly, the steric hindrance around the metal center can also be adjusted. Tolman introduced the cone angle θ in order to compare the steric effects of different substituents on the phosphines.²⁷ By varying alkyl groups on the phosphorus, the steric properties of the donor groups can be altered without much change in the corresponding electronic properties.

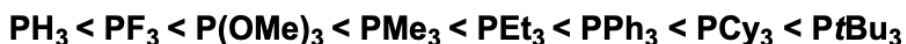


Figure 4 Tolman cone angle

As phosphorus is monoisotopic and has a nuclear spin of $\frac{1}{2}$, reactions can also easily be monitored by ^{31}P NMR spectroscopy. Since signals from coordinated phosphines usually are significantly shifted downfield from the free ligand, this method is ideal to characterize complexes and for reaction control.

1.4. PCP Pincer Complexes

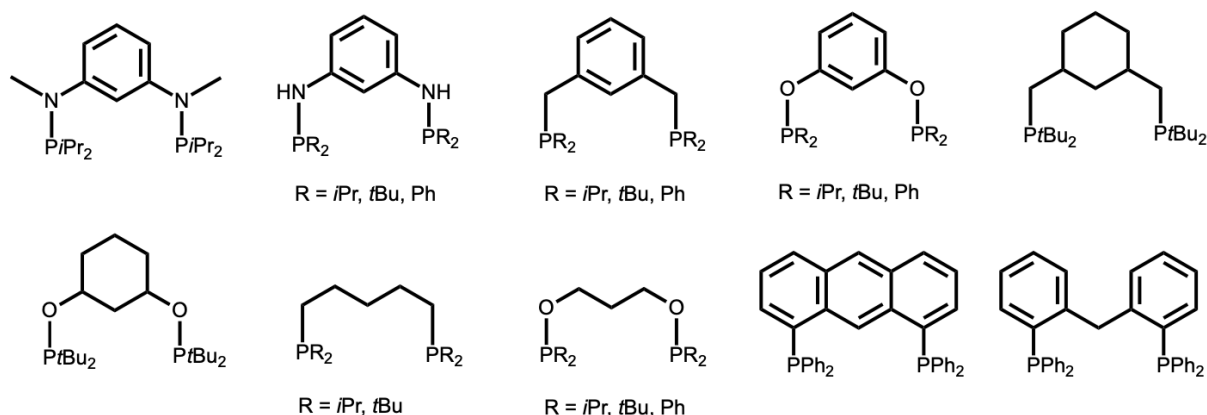


Figure 5 Examples of PCP pincer ligands

The first complexes bearing PCP ligands were published by Moulton and Shaw in 1976.²⁸ They reported a series of complexes starting from Ni, Pd, Pt, Rh and Ir precursors. Initially, however, research on PCP pincer complexes remained relatively limited, until a series of PCP pincer complexes, mainly with metals of the second and third transition row, showed promising applicability as catalysts in the late 1990s.²⁹⁻³³ This greatly increased interest in this type of complexes.³⁴

PCP complexes with base metals, however, are still exceedingly rare. The vast majority of them being comprised of Ni complexes. Nevertheless, recently the synthesis of PCP pincer complexes with Co, Fe, Mn, Cr, Mo and W has also been reported.

1.4.1. Group 10 PCP pincer complexes

The first PCP-group 10 complexes were synthesized by Moulton and Shaw in 1976. They were prepared by refluxing a CH_2 -linked PCP ligand with the corresponding metal-chloride precursors in alcohols, with short reaction times of 5 to 25 min. The corresponding Ni, Pd and Pt complexes were, however, only obtained in moderate

yields of 32 to 75 %. These complexes proved to be very stable. In fact, they did not decompose in air at temperatures of up to 295 °C and could therefore be purified by sublimation.²⁸

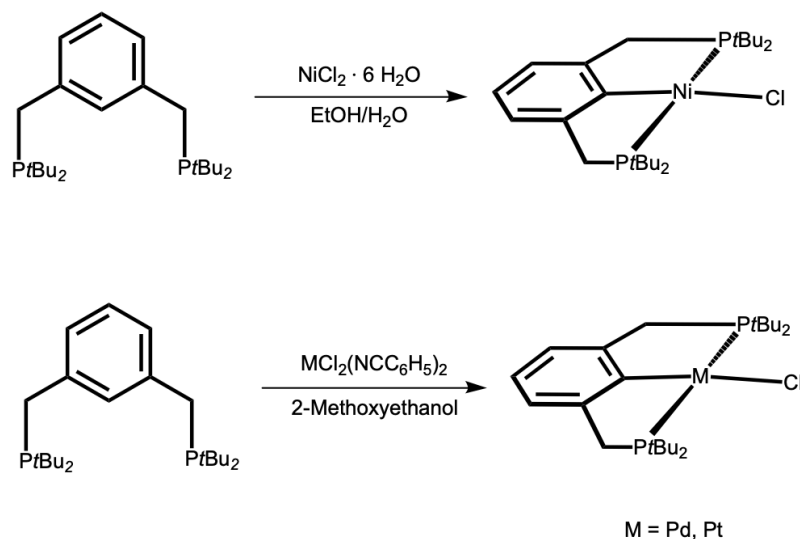


Figure 6 First synthesis of group 10 PCP pincer complexes

Even though they were among the first pincer complexes ever to be synthesized, so far, only few applications of PCP-Pt complexes have been reported. They are limited to few reports of CO_2 and CO activation as well as one report of a Pt-PCP catalyzed hydroamination of acrylonitrile.³⁵⁻³⁷ Due to the poor solubility and low reactivity of common Pt precursors, the yields of the complexations were usually poor. However, by addition of base or usage of an internal base in precursors, it was possible to enhance them to similar levels as reported for the other group 10 metals.^{6,38}

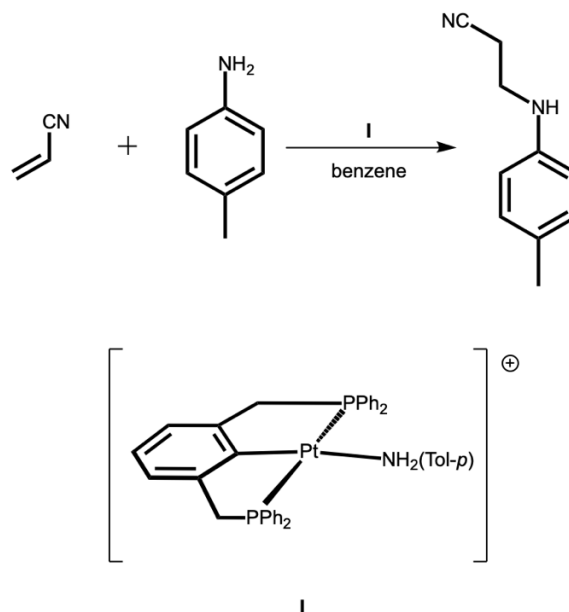


Figure 7 Pt-catalyzed hydroamination of acrylonitrile

Milstein showed in 1997 that PCP-Pd pincer complexes effectively catalyze Heck coupling reactions. He compared the reactivity of pincer ligands that form sp^2 as well as sp^3 Pd-C bonds and determined that the sp^3 bonded PCP-Pd complex **III** showed higher turnover numbers (TON). He attributed the higher reactivity to the higher electron density at the Pd center of the sp^3 hybridized complex.³¹ Indeed, work by Sjövall, in 2002 showed that the reactivity could be increased even more when using a fully aliphatic PCP pincer **IV**.³⁹ In 2000 Bedford showed that PCP-Pd pincer complexes were also effective in catalyzing Suzuki-Miyaura reactions, thus showing their applicability in cross coupling reactions.⁴⁰

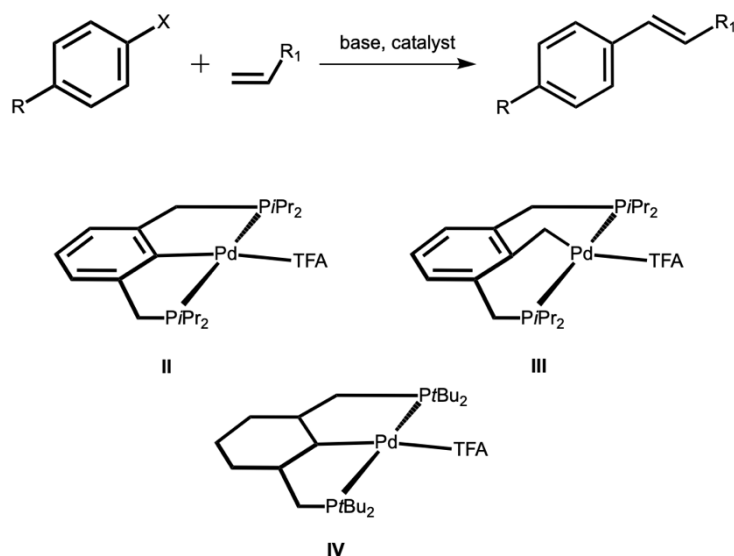


Figure 8 Heck reaction with PCP-Pd complexes

The catalytic cycle of Heck-couplings usually involves Pd(0) complexes that are transformed via oxidative addition of aryl halides to Pd(II) complexes, consequently after elimination of the final product the Pd(0) species is regenerated by reductive elimination of hydrogen halide, aided by base. However, attempts to reduce the PCP-Pd(II) pinners to the corresponding Pd(0) compounds were unsuccessful without decomposition, as these complexes proved to be too stable. Therefore, Milstein and Jensen proposed a catalytic cycle that indicates a progression from Pd(II) to Pd(IV) and back to Pd(II), under the assumption that the palladium-carbon bond was too strong to be broken in the catalytic conditions.^{31,32} This cycle however remains controversial, because, as of yet, no experimental evidence of any Pd(IV) species was reported.⁴¹

Kinetic studies and catalyst poisoning experiments indicated that decomposition of the pincer complexes into colloidal Pd(0) nanoparticles, catalyzing the reactions, can take place. It is assumed that the stability of the complexes directly influences its reactivity. Less stable systems, like phosphinite pinners decompose faster, thus increasing the reactivity. It was further concluded that trialkyl amines, used as base in the reactions, are responsible for the decomposition, as the complexes veritably show high stability at the temperatures used for the reactions.⁴² In cross coupling reactions, however, under mild conditions, some evidence, like full catalyst recovery and negative Pd(0) poisoning tests, plausibly hints to Pd(II) to Pd(IV) cycles.⁴³

In analogy to the corresponding PCP-Pd pincers, PCP-Ni pincers have shown reactivity in cross coupling reactions. Complex **V** showed to effectively catalyze the Suzuki-Miyaura reaction, albeit entailing higher reaction temperatures and higher catalyst loadings than similar Pd complexes. The formation of Ni-nanoparticles was observed in this reaction.⁴⁴

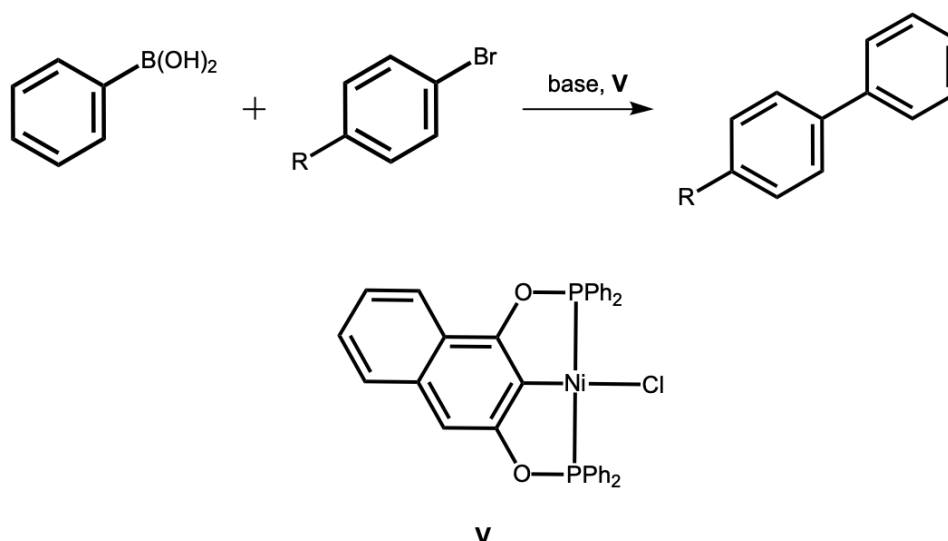


Figure 9 PCP-Ni catalyzed Suzuki-Miyaura reaction

Furthermore, other catalytic applications catalyzed by PCP-Ni complexes, like C-S cross coupling, hydrosilylation or hydroamination of nitriles, are also known in literature.³⁴

The first PCP-Ni complexes possessing amine linking groups were reported by the Kirchner group in 2006. They were prepared by refluxing a 1,3-diaminobenzene-based PCP pincer ligand with $\text{NiCl}_2 \cdot 6\text{H}_2\text{O}$ in ethanol.⁶

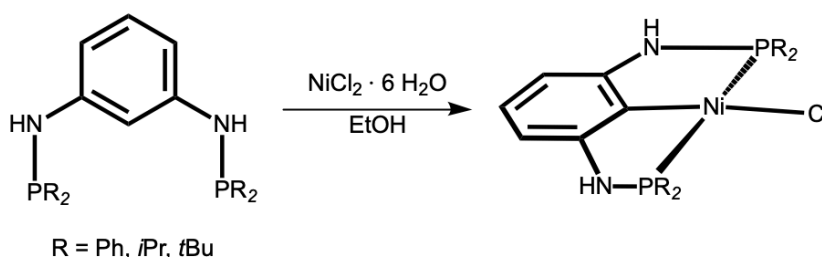


Figure 10 Synthesis of PCP-Ni complex

As the NH linkers proved to be acidic, Murugesan used N-methylated linkers in order to make the complexes compatible with strong base, which allowed for access to new reactions.⁸ For example, the Ni(II) borohydride complex $[\text{Ni}(\text{PCP}^{\text{NMe}})(\eta^2\text{-BH}_4)]$ was successfully synthesized via two different methodologies. Firstly, by reacting the PCP-Ni halide complex directly with NaBH_4 in a mixture of THF/MeOH. The second approach included the reaction of the halide complex with LiAlH_4 to generate the hydride complex. $[\text{Ni}(\text{PCP}^{\text{NMe}})\text{H}]$ was then treated at RT with $\text{BH}_3\cdot\text{THF}$, also generating the borohydride complex. Treating $[\text{Ni}(\text{PCP}^{\text{NMe}})(\eta^2\text{-BH}_4)]$ with TEA regenerated the hydride complex.⁹

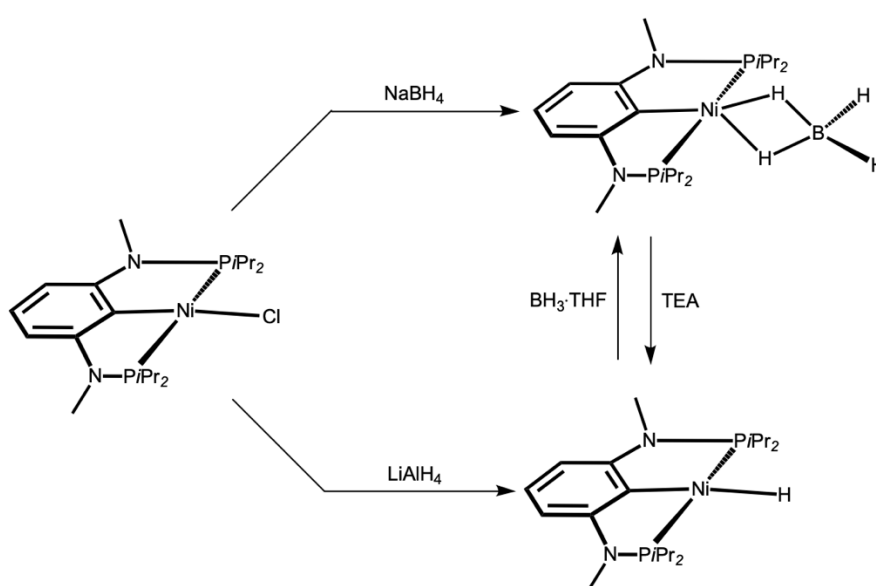


Figure 11 Preparation on PCP-Ni borohydride complexes

The hydride and borohydride Ni complexes are able to react with gaseous CO_2 , thus creating the inserted formate complexes.^{34,45}

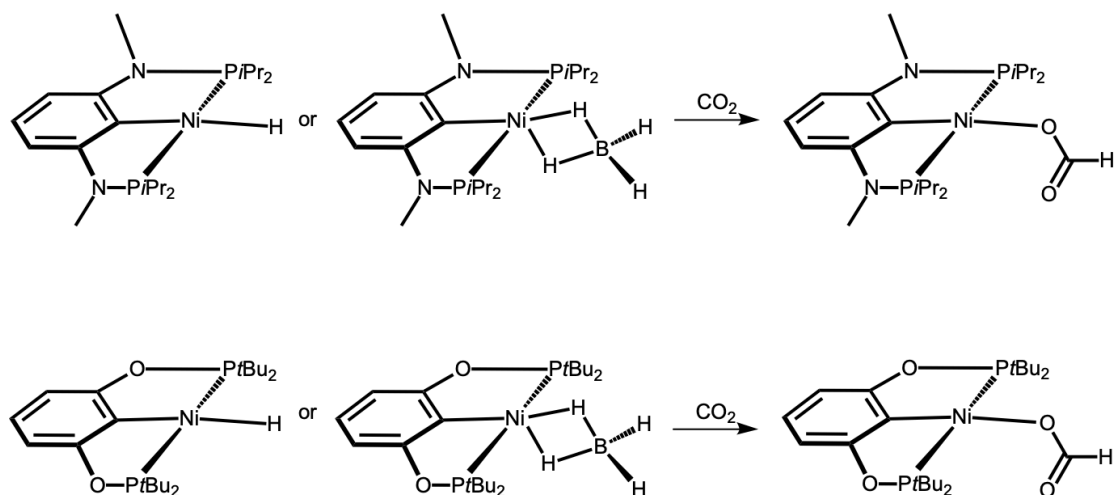


Figure 12 Activation of CO_2 by PCP-Ni complexes

1.4.2. Group 9 PCP Pincer Complexes

The first PCP-Rh and PCP-Ir complexes were prepared by Moulton and Shaw by treating the respective metal(III) chlorides with PCP ligand in a mixture of water and isopropyl alcohol and refluxing this mixture for 20 h. The corresponding metal hydride PCP complexes were obtained in yields of about 70 %.²⁸

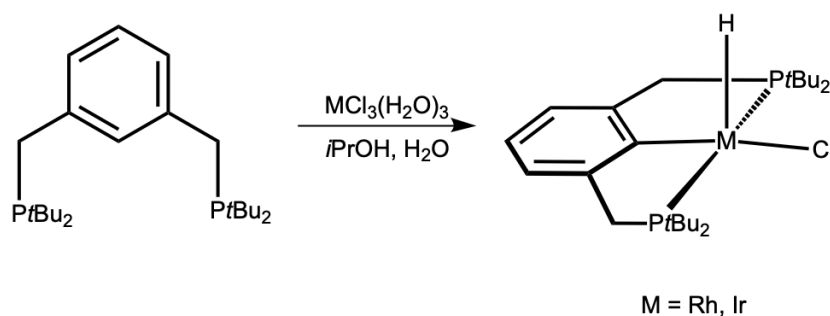


Figure 13 Synthesis of Rh and Ir PCP pincer complexes

PCP-Ir complexes have proved to be impressive catalysts in the dehydrogenation of alkanes to alkenes. In 1996, Gupta reported the dehydrogenation of cyclooctane to cyclooctene with dihydride Rh and Ir PCP complexes. The PCP-Ir complexes were far more reactive than their Rh analogues and additionally proved to be exceptionally

stable at the high temperatures needed for the reaction. No decomposition of the catalyst occurred at temperatures of 200 °C for as long as a week. The activity of the catalyst was further increased by using a hydrogen acceptor such as *tert*butyl ethylene.²⁹

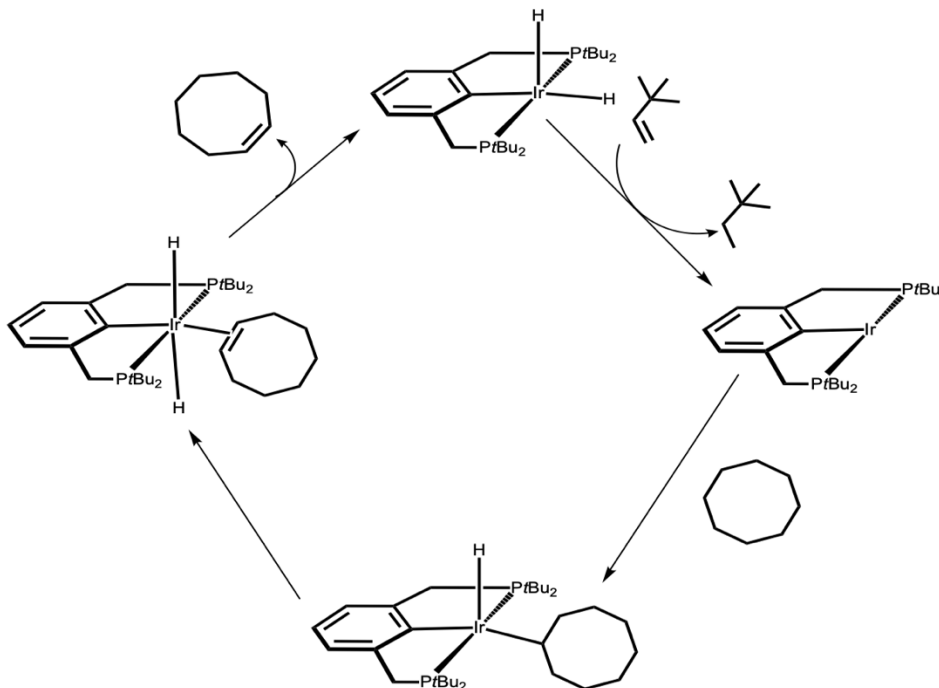


Figure 14 Catalytic cycle for the dehydrogenation of an alkane by PCP-Ir complexes

The catalytic cycle includes CH activation of the alkane, followed by β -hydride elimination, liberation of the alkene and dehydrogenation of the formed dihydride complex in the presence of a hydrogen acceptor.⁴⁶ In 2006 Goldman reported the metathesis of alkanes, utilizing PCP-Ir complexes for hydrocarbon hydrogenation/dehydrogenation reactions, combined with Schrock-type olefin metathesis catalysts.⁴⁷

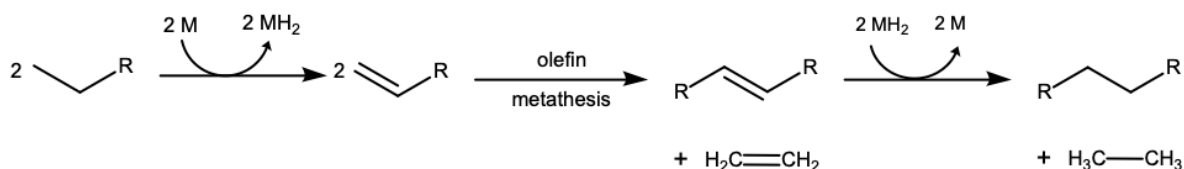


Figure 15 Ir catalyzed alkane metathesis described by Goldman

PCP-Rh complexes have been used to a lesser degree as catalysts, compared to their Ir analogues. However, their applications include amongst others the decarbonylation of aldehydes and acyl compounds, the carbonylation of methanol, as well as coupling reactions.⁴⁸⁻⁵⁰

An interesting feature of Rh is that it can insert into strong, unstrained C-C bonds. When reacting Rh alkene precursors in oxidative addition reactions with a PCP ligand containing an arene-methyl bond on the *ipso* position, a PC(sp²)P-Rh-methyl complex instead of the expected PC(sp³)P-Rh-hydride complex is formed. This reaction even takes place at room temperature.⁵¹

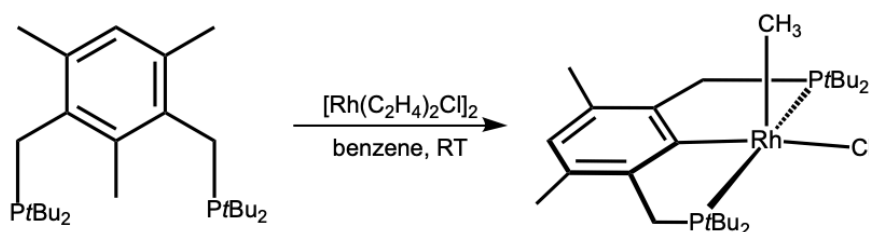


Figure 16 C-C bond activation in PCP-Rh complexes

The first PCP-Co complexes were synthesized by Li and coworkers in 2009.⁵² They reacted the aliphatic PCP ligands (Ph₂POCH₂)₂CH₂ with the electron rich cobalt precursor Co(Me)(PMe₃)₄ and obtained the corresponding PC(sp³)P-Co(I) complex. Methane was liberated during the reaction. This complex was then treated with MeI leading to oxidative addition and formation of a Co(III) complex.

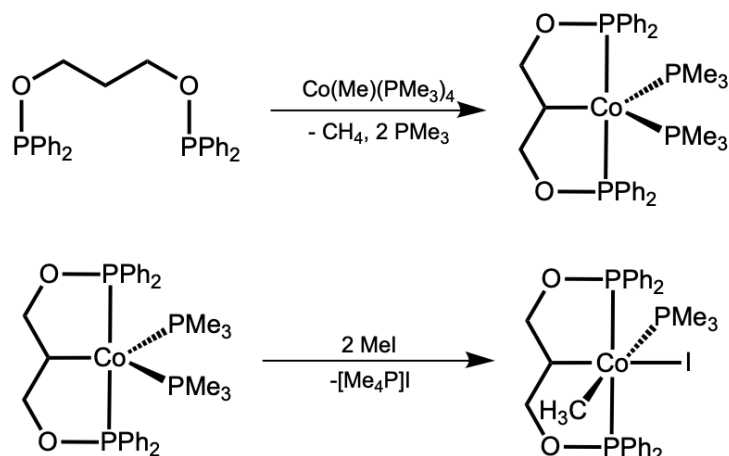


Figure 17 Synthesis of the first PCP-Co complexes

The first PC(sp²)P-Co complex was prepared by Li in 2010 by treating a POCOP ligand with Co(PMe₃)₄ in Et₂O and stirring it at room temperature for 48 h, generating the trigonal-bipyramidal PCP-Co(I) complex **VI** with a yield of 30 %.⁵³

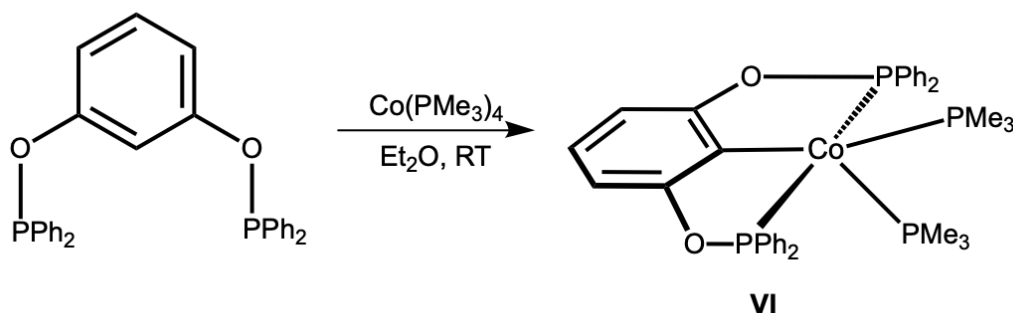


Figure 18 Synthesis of [Co(POCOP)(PMe₃)₂]

Later, the Kirchner group reported the synthesis of a series of novel PCP-Co complexes using the 1,3-diaminobenzene-based ligand.

Treatment of the ligand with *n*-BuLi and subsequent reaction with anhydrous CoCl₂ yielded the square planar low spin PCP-Co complex **VII** in near quantitative yield.

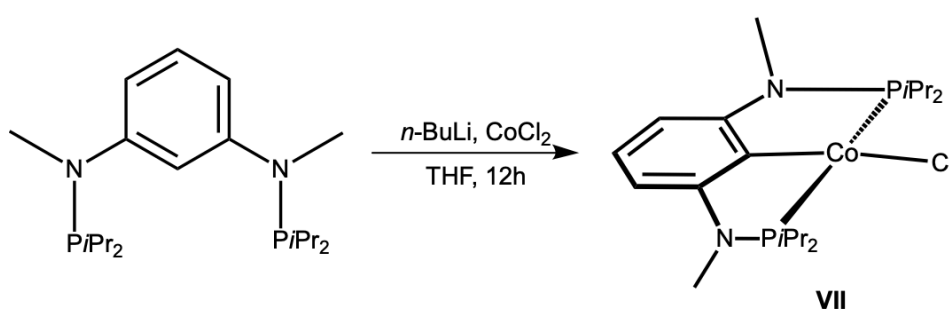


Figure 19 Synthesis of [Co(PCP^{NMe})Cl]

Directly treating **VII** with either CO or pyridine affords the square-pyramidal complexes [Co(PCP^{NMe})(CO)Cl] (**VII a**) and [Co(PCP^{NMe})(py)Cl] (**VII b**) respectively. By using halide scavengers such as AgSbF₆ in presence of CO, the cationic trigonal-bipyramidal complex **VII c** [Co(PCP^{NMe})(CO)₂]⁺SbF₆⁻ is formed. **VII** can be oxidized with

CuCl_2 to the Co(III) species $[\text{Co}(\text{PCP}^{\text{NMe}})\text{Cl}_2]$ (**VII d**). Reducing **VII** with KC_8 under CO atmosphere affords the diamagnetic Co(I) complex **VII e** $[\text{Co}(\text{PCP}^{\text{NMe}})(\text{CO})_2]$.⁸

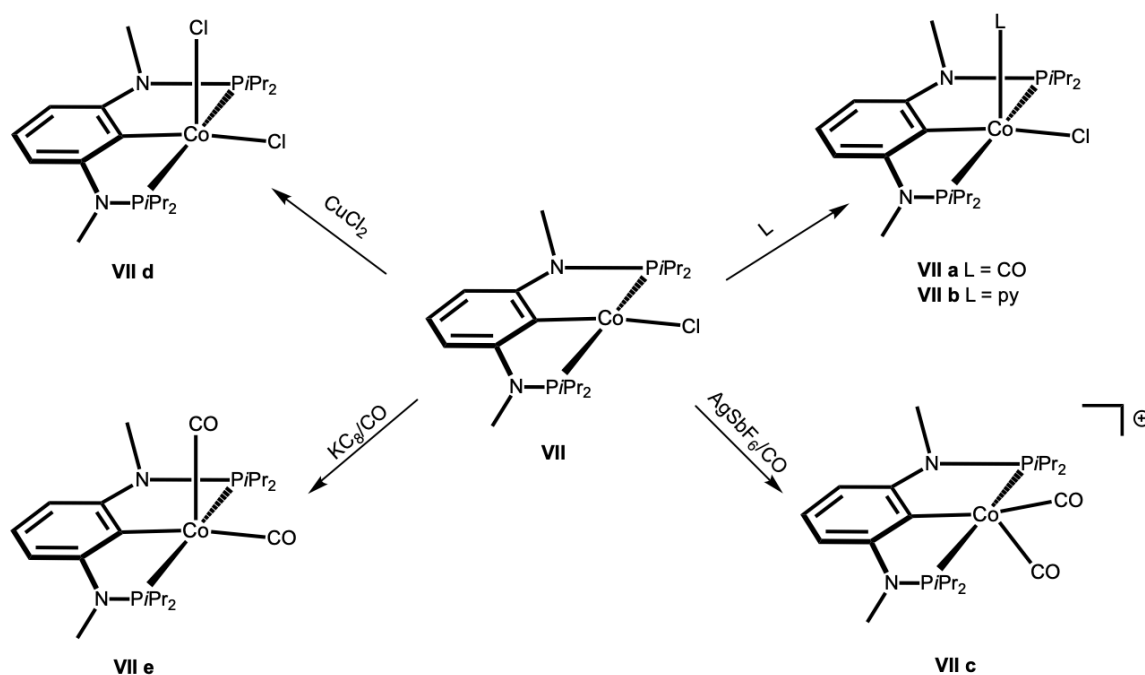


Figure 20 Reactions of $[\text{Co}(\text{PCP}^{\text{NMe}})\text{Cl}]$

VII also proved to be an effective catalyst for the coupling of primary alcohols with aromatic amines. The coupling involves acceptorless dehydrogenation of the alcohol and formation of an imine, which subsequently is hydrogenated to the amine. (borrowing hydrogen catalysis).⁵⁴

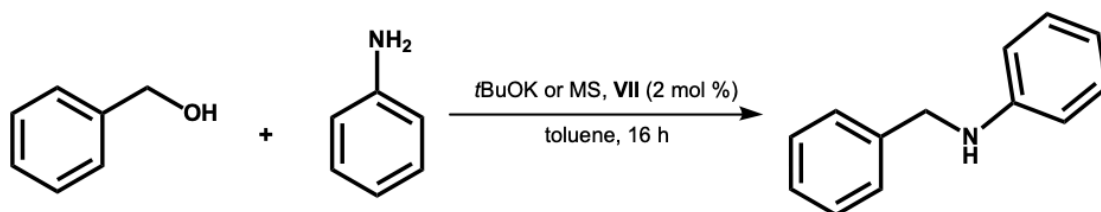


Figure 21 PCP-Co catalyzed coupling of primary alcohols with aromatic amines

Analogous to the square planar PCP-NiCl complexes, treatment of **VII** with NaBH_4 yielded the borohydride complex $[\text{Co}(\text{PCP}^{\text{NMe}})(\eta^2\text{-BH}_4)]$ (**VII f**). However, due to its high

stability, the complex showed neither reactivity towards CO_2 nor was it possible to create a hydride complex by treatment with TEA.⁹

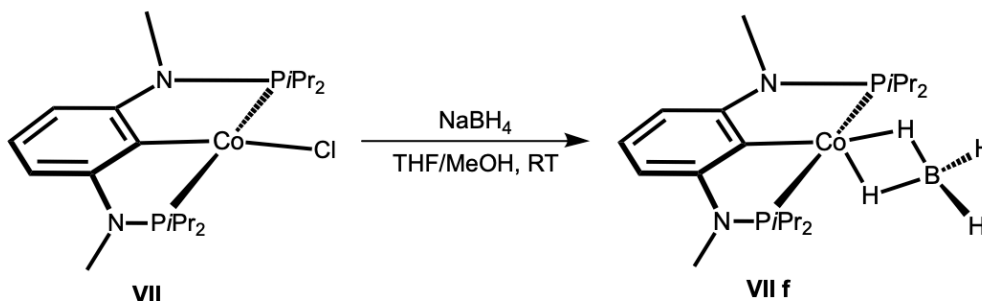


Figure 22 Synthesis of $[\text{Co}(\text{PCP}^{\text{NMe}})(\eta^2\text{-BH}_4)]$

1.4.3. Group 8 PCP Pincer Complexes

The first $\text{PC}(\text{sp}^3)\text{P-Os}$ complex was synthesized by Roper and coworkers in 1984, by two successive electrophilic additions of a Fischer carbene on two PPh_3 ligands.⁵⁵

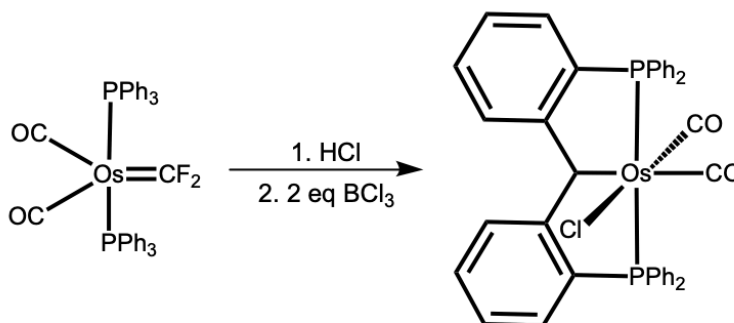


Figure 23 Synthesis of the first $\text{PC}(\text{sp}^3)\text{P-Os}$ complex

A first $\text{PC}(\text{sp}^2)\text{P}$ complex was reported by Jia in 2000. It was prepared by refluxing $\text{OsCl}_2(\text{PPh}_3)_3$ with PCP ligand in isopropanol for 8 h, giving the corresponding square-pyramidal $\text{Os}(\text{II})$ complex $[\text{Os}(\text{PCP})(\text{PPh}_3)\text{Cl}]$ in 65 % yield.⁵⁶

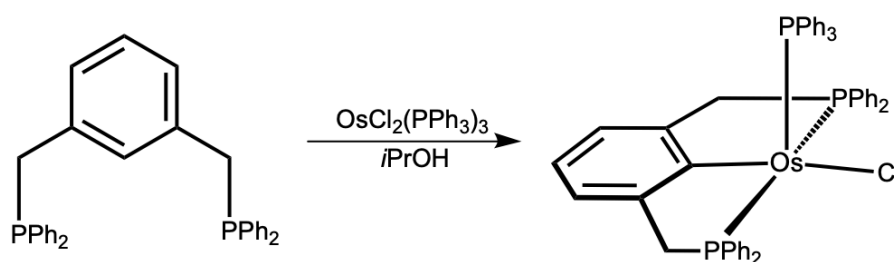


Figure 24 Synthesis of the first $PC(sp^2)P$ -Os complex

Cyclooctene hydride PCP-Os pincer complexes ($[Os(PCP)(COE)H]$), bearing CF_3 moieties bonded on the phosphine donors, can be used for dehydrogenation reactions of alkanes. They show comparable reactivity to the CH_2 linked $[Ir(PCP^{tBu})H_2]$ complexes. Ir-dihydride complexes utilizing POCOP ligands, however, significantly outperform these Os catalysts.⁵⁷

By treating $RuCl_2(PPh_3)_4$ with a PCP ligand and refluxing it in CH_2Cl_2 for 3 days, van Koten prepared the first PCP-Ru pincer **VIII** in 1996 in a yield of 58 %.⁵⁸

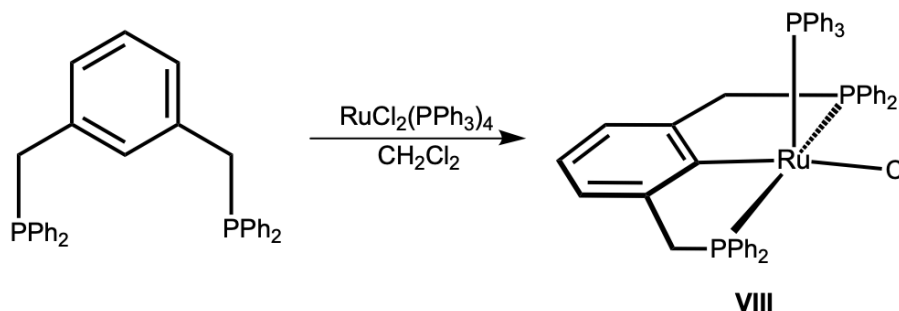


Figure 25 Synthesis of the first PCP-Ru complex

Four years later, van Koten described the reactivity of **VIII** as hydrogen-transfer catalyst for ketones. By using isopropanol as a reducing agent and with low catalyst loadings of 0.1 %, turnover frequencies (TOF) of up to $10,000\ h^{-1}$ for the reduction of cyclohexanone were achieved.³³

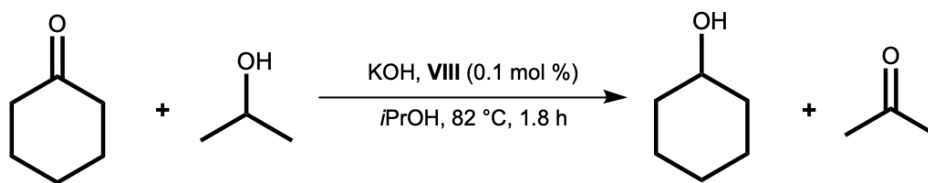


Figure 26 Transfer hydrogenation of cyclohexanone with a PCP-Ru complex

After treating the complex $[\text{Ru}(\text{PCP}^{\text{OH}})(\text{CO})_2\text{Cl}]$ **IX** with base or proton sponge, Milstein discovered the first metallaquinone **IXa** in 2000. In this ruthenaquinone the second oxygen of the quinone is replaced by the metal. The bond lengths of the ring, as well as the length of the O-C bond correspond to the lengths expected in the more traditional, organic benzoquinone.⁵⁹

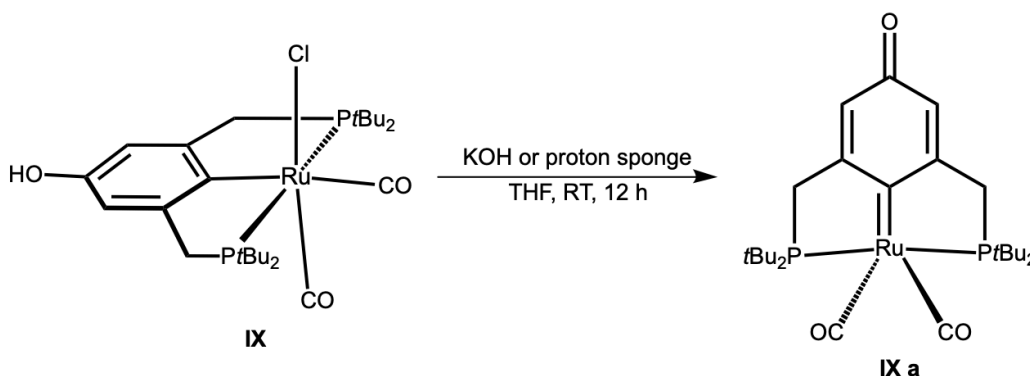


Figure 27 First synthesis of a metallaquinone

Simultaneously with the first PCP-Co complex, Ji and coworkers also published the synthesis of the first PCP-Fe complex in 2009. By reacting the ligand $(\text{Ph}_2\text{POCH}_2)_2\text{CH}_2$ with the Fe precursor $\text{Fe}(\text{Me})_2(\text{PMe}_3)_4$ in diethyl ether the PCP-Fe hydride complex **X** was formed.

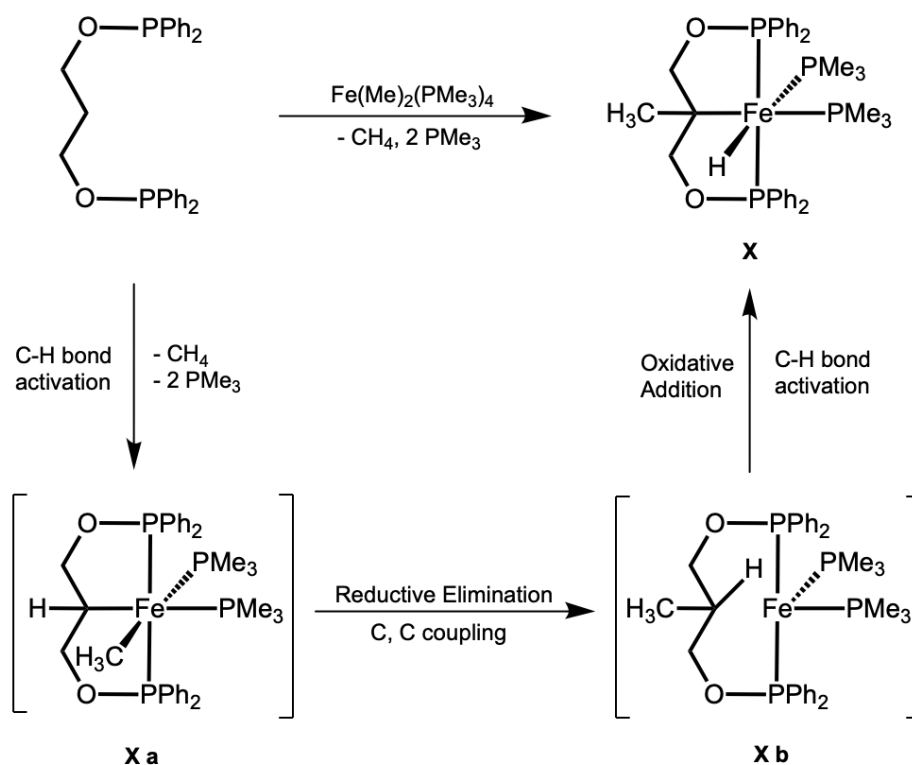


Figure 28 Synthesis of the first PCP-Fe complex

The unusual complexation mechanism is initiated with pre-coordination of the phosphines and loss of two PMe_3 ligands. Then the sp^3 C-H bond of the ligand is activated, which in turn leads to elimination of methane generating transition state **Xa**. Thereafter, C, C coupling between the methyl ligand and the *ipso* carbon occurs, and after reductive elimination, the Fe(0) transition state **Xb** is formed. The C, C coupling reaction hereby induces a change of the backbone of the ligand. Finally, after another C-H bond activation and oxidative addition the $\text{PC}(\text{sp}^3)\text{P}-\text{Fe}(\text{II})$ complex **X** is obtained.⁵²

In 2011, Guan reported the first synthesis of a $\text{PC}(\text{sp}^2)\text{P}-\text{Fe}$ complex via oxidative addition of resorcinol-bis(phosphinite) ligands on a $\text{Fe}(\text{PMe}_3)_4$ precursor in THF. The reaction yields of the $\text{POCOP}-\text{Fe}(\text{II})\text{H}$ (**XI a**) pincers were 69 % for the phenyl and 67 % for the isopropyl phosphine substituents, respectively. When using the bulkier *tert*-butyl phosphine donating groups, however, only trace amounts of the corresponding complex were observed, indicating that steric crowding around the metal center does inhibit the reaction.

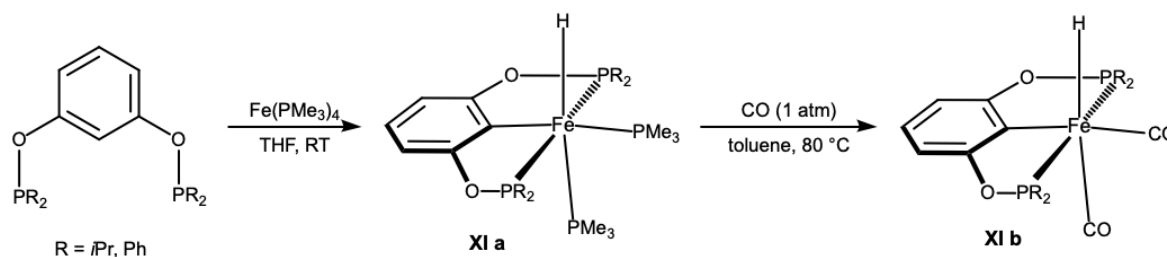


Figure 29 Synthesis of POCOP-Fe hydride complexes

By heating complexes **XI a** under CO atmosphere for three days at 80 °C, the dicarbonyl complexes **XI b** were obtained. Furthermore, Guan reported that the complexes **XI a** showed reactivity as catalyst for the hydrosilylation of ketones to alcohols.⁶⁰

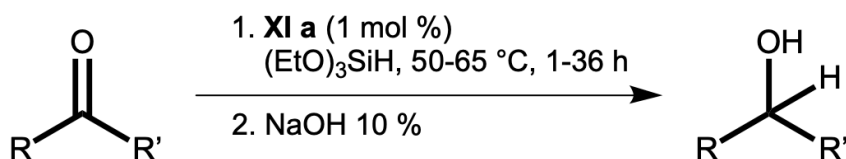


Figure 30 Hydrosilylation of ketones with PCP-Fe complexes

Later, Sortais and Milstein described the synthesis of PCP-Fe(II) complexes with NH₂, and CH₂ linkers respectively. They obtained the complexes by reacting Fe(CO)₅ with the respective ligands under ultraviolet radiation.^{61, 62}

In 2017, in analogy to the ruthenaquinone complex **IX a**, Milstein reported the synthesis of the corresponding ferraquinone complex by treatment of [Fe(PCP^{OH})(CO)₂H] with benzoquinone.

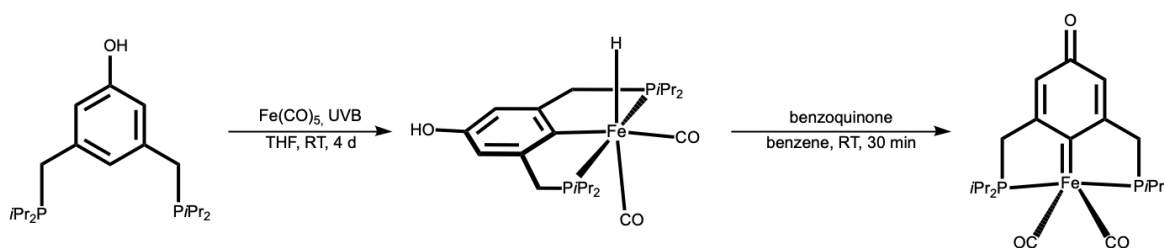


Figure 31 Synthesis of the first ferraquinone complex

The Kirchner group reported the synthesis of PCP-Fe complexes in 2018. By using a PCP ligand with a chlorine substituent on the *ipso*-position, complex **XII** $[\text{Fe}(\text{PCP}^{\text{NEt}})(\text{CO})_2\text{Cl}]$ was synthesized under solvothermal conditions, by means of oxidative addition on $\text{Fe}_2(\text{CO})_9$. In a next step, with the aim of creating a hydride species, complex **XII** was treated with Lithium triethylborohydride ($\text{Li}[\text{HBET}_3]$). However, no hydride species was observed, only the unusual 17 electron Fe(I) complex **XIIa** $[\text{Fe}(\text{PCP}^{\text{NEt}})(\text{CO})_2]$ was isolated.

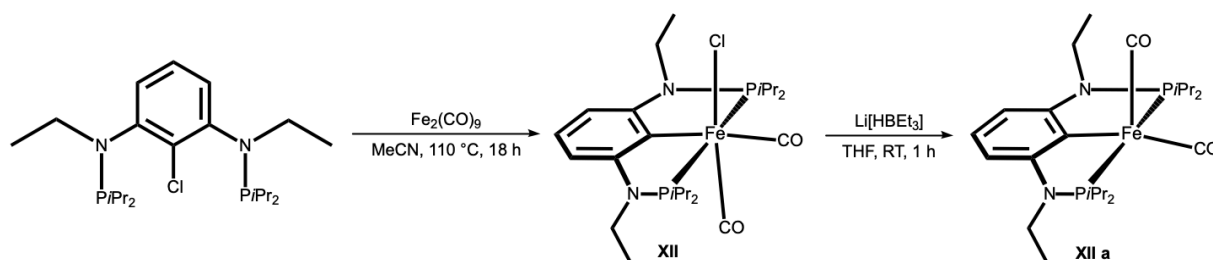


Figure 32 Preparation of $[\text{Fe}(\text{PCP}^{\text{NEt}})(\text{CO})_2\text{Cl}]$ and $[\text{Fe}(\text{PCP}^{\text{NEt}})(\text{CO})_2]$

Stirring **XIIa** under NO atmosphere gave the diamagnetic complex **XIIb** $[\text{Fe}(\text{PCP}^{\text{NEt}})(\text{CO})(\text{NO})]$, a rare example of a nitrosyl PCP complex.⁶³

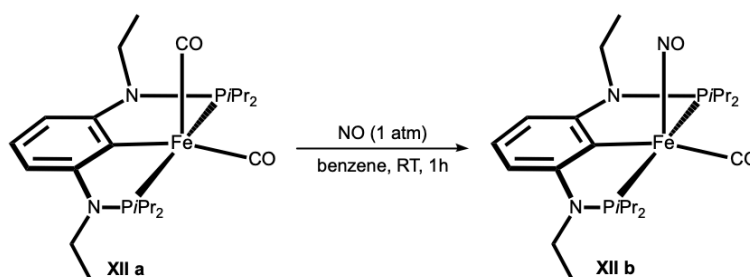


Figure 33 Synthesis of $[\text{Fe}(\text{PCP}^{\text{NEt}})(\text{CO})(\text{NO})]$

1.4.4. Group 7 PCP Pincer Complexes

In contrast to the groups 8, 9 and 10, the PCP pincer complexes of group 7 metals are as of yet extremely rare and research on their chemical properties, complexation methods and applications started only very recently.

The first PCP-Re complexes were reported by Ozerov and co-workers in 2016. By reacting the Re(V) precursor $(\text{Me}_2\text{S})_2\text{ReOCl}_3$ with PCP ligand in acetonitrile he first observed a precipitate that he tentatively characterized as the non-cyclometalated adduct $[\text{Re}(\text{PC}(\text{H})\text{P})\text{OCl}_3]_n$ (**XIII**). When conducting the reaction in toluene, the PCP-Re(V) pincer $[\text{Re}(\text{PCP})\text{OCl}_2]$ (**XIIIa**) was formed in 51% yield, after heating the adduct **XIII** with TEA as base at 140 °C for 48 h. Treatment of **XIIIa** with LiAlH_4 and quenching the reaction with water yielded the Re(I) polyhydride complex $[\text{Re}(\text{PCP})\text{H}_6]$ (**XIIIb**). By stirring **XIIIb** for 24 h at room temperature under CO atmosphere the Re(I) complex $[\text{Re}(\text{PCP})(\text{CO})_3]$ (**XIIIc**) was afforded.⁶⁴

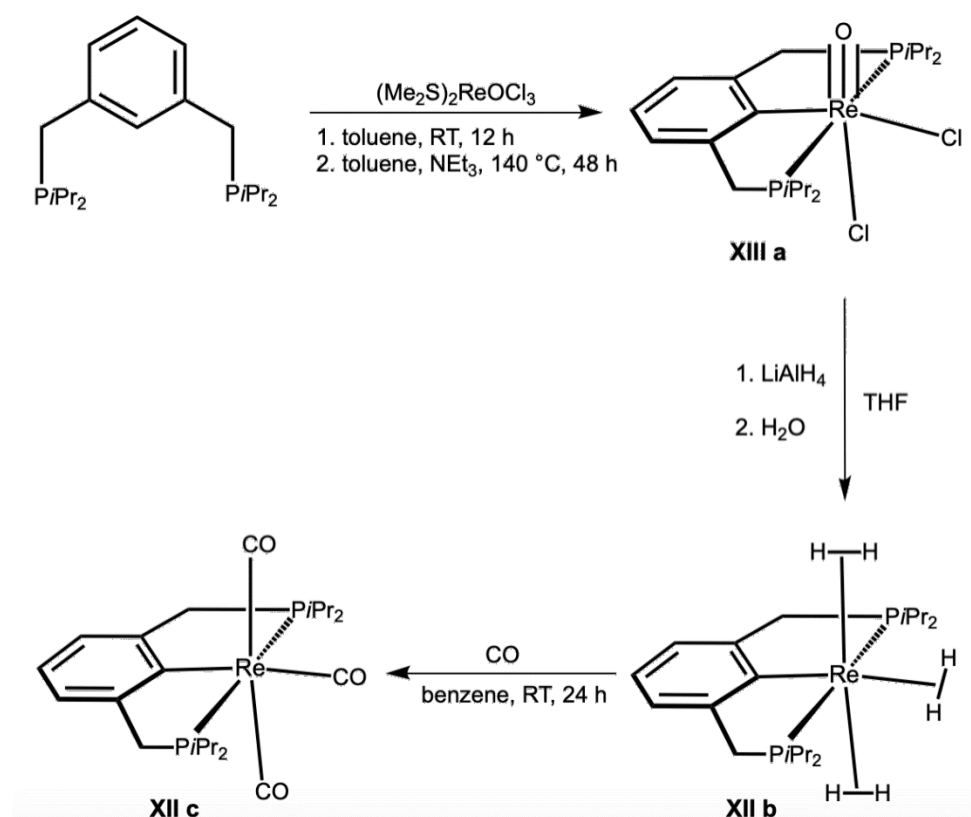


Figure 34 Synthesis of PCP-Re pincers

By treating complex **XIII a** with the strong base lithium hexamethyldisilamide (LiHMDS) it was possible to successfully abstract a proton from the CH_2 linking group, hereby dearomatizing the benzene backbone. This marked the first time that the deprotonation of a CH_2 -linker was achieved in PCP pincer complexes.⁶⁵

The first PCP-Mn pincer complex was synthesized by the Kirchner group in 2018. For the reaction, a PCP ligand with a 1,3-diaminobenzene backbone was used. In anticipation of facilitating oxidative addition reactions, the hydrogen atom on the *ipso*

carbon was exchanged with a chlorine substituent. The ligand was reacted with $\text{Mn}_2\text{CO}_{10}$ in acetonitrile under solvothermal conditions, i.e. in a sealed glass vial at temperatures above the boiling point of the used solvent. The novel PCP-Mn pincer $[\text{Mn}(\text{PCP}^{\text{NEt}})(\text{CO})_3]$ (**XIII**) was obtained in 40 % yield.

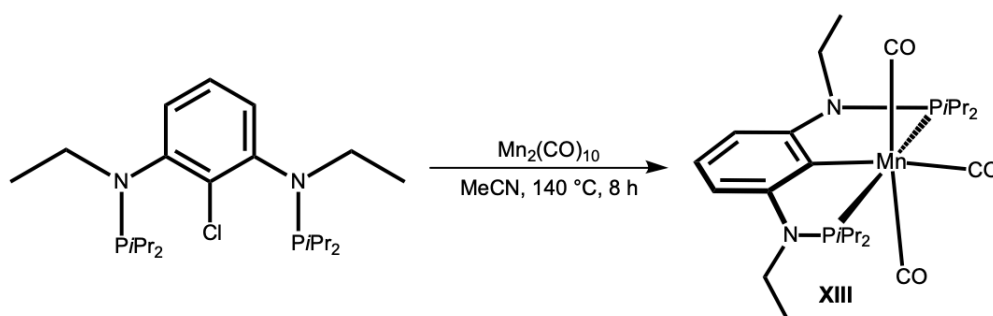


Figure 35 Synthesis of the first PCP-Mn complex

The CO ligands of the complex proved to be inert to ligand substitution, no reaction with CNTBu was observed, even under elevated temperatures. However, reacting **XIII** with NOBF_4 led to replacement of one CO ligand with NO, affording the cationic Mn(I) complex $[\text{Mn}(\text{PCP}^{\text{NEt}})(\text{CO})_2(\text{NO})]\text{BF}_4$ (**XIIIa**).

It was also possible to obtain a complex $[\text{Mn}(\text{PC}(\text{H})\text{P}^{\text{NEt}})(\text{CO})_3]\text{BF}_4$ featuring an agostic $\eta^2\text{-C}_{\text{aryl}}\text{-H}$ bond. This was achieved via protonation of the *ipso* C-Mn bond with $\text{HBF}_4 \cdot \text{Et}_2\text{O}$ (**XIIIb**). The reaction proved to be reversible and even weak bases such as TEA were able to deprotonate the agostic C-H bond thereby regenerating **XIII**.⁶⁶

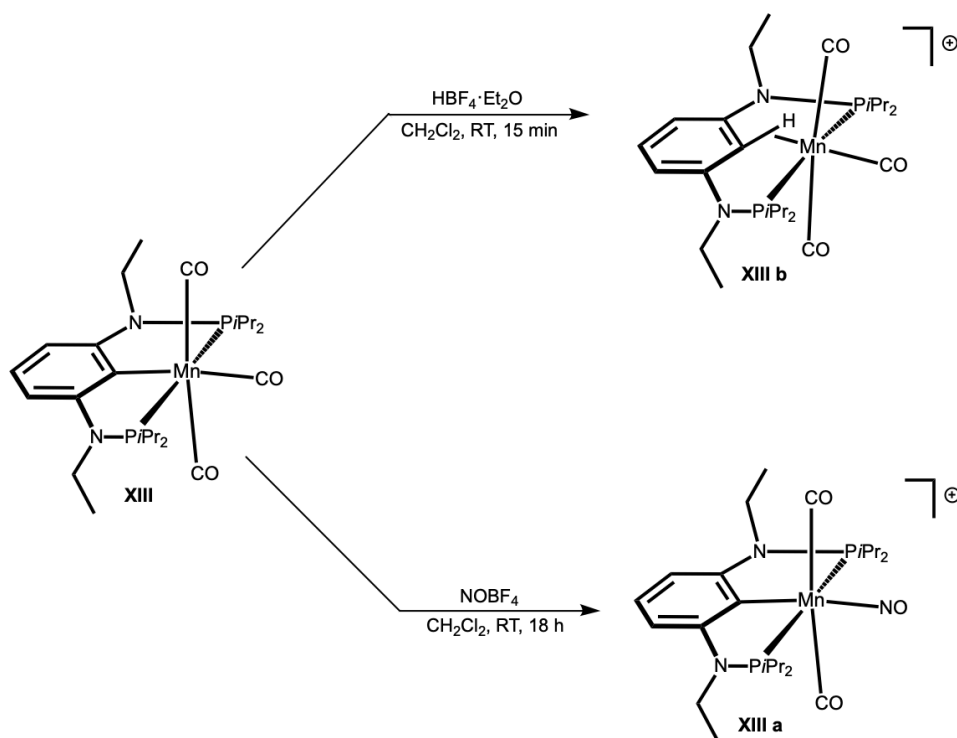


Figure 36 Reactions of $[\text{Mn}(\text{PCP}^{\text{NEt}})(\text{CO})_3]$

1.4.5. Group 6 PCP Pincer Complexes

Analogous to group 7 metals, examples of PCP pincer complexes of the group 6 metals are hardly known in literature and research on them started only very recently. The Kirchner group reported the reaction of the group 6 carbonyl complexes with a 1,3-diaminobenzene based PCP pincer under solvothermal conditions in 2016. However, Cr and Mo only formed agostic pseudo pincer complexes, containing an $\eta^2\text{-C}_{\text{aryl}}\text{-H}$ bond (**XIV**, **XV**). W was however able to cleave the *ipso* C-H bond and formed the desired capped octahedral complex $[\text{W}(\text{PCP}^{\text{NMe}})(\text{CO})_3\text{H}]$ (**XVI**), the first PCP-W complex reported in literature.¹¹

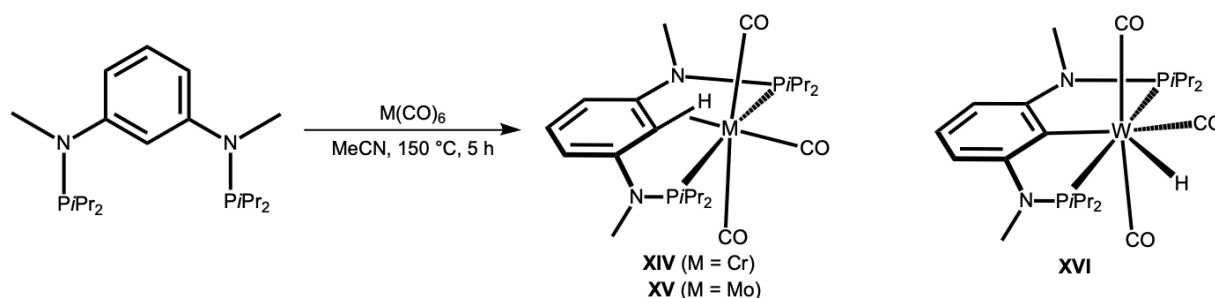


Figure 37 Synthesis of the first PCP-W complex

The first PCP-Mo complex was synthesized by Schrock in 2012 in his work on dinitrogen-cleavage using single metal centers. In this work he reacted the POCOP ligand 1-iodo-2,6-[OP(*t*Bu)₂]₂C₆H₃ with *n*-BuLi and transmetalated the PCP-Li species with MoCl₃(THF)₃. He obtained the desired square-pyramidal Mo(III) pincer **XVII** [Mo(POCOP)I₂] in 46 % yield but also observed 10-15 % of a diamagnetic impurity, which he proposed as being the Mo(V)oxo complex **XVIIa** [Mo(POCOP)(O)I]. He based this assumption on the known property of the precursor MoCl₃(THF)₃ to decompose and give molybdenum-oxo species.

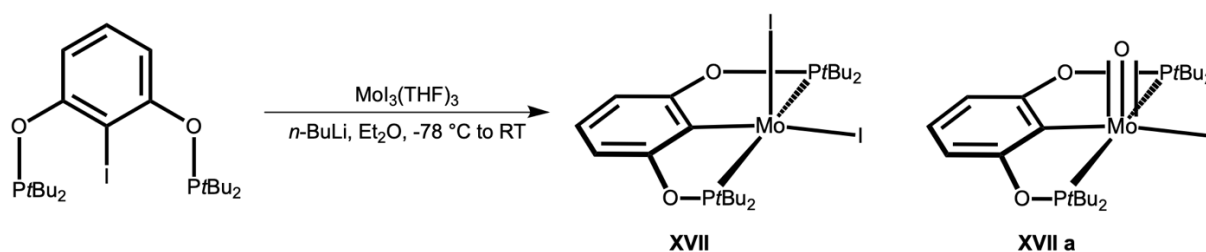


Figure 38 Synthesis of [Mo(POCOP)I₂] and [Mo(POCOP)(O)I]

Reducing the mixture of complexes **XVII** and **XVIIa** under a N₂ atmosphere with Na/Hg in the presence of crown ether gave the anionic nitrido species [Mo(POCOP)(N)]⁻ **XVIIb**. Attempts to protonate the nitride to yield the neutral imido complex failed. Instead the diamagnetic complex **XVIIc** was formed. Based on NMR spectroscopy, Schrock proposed that in this complex a protonation of the Mo-P bond took place.⁶⁷

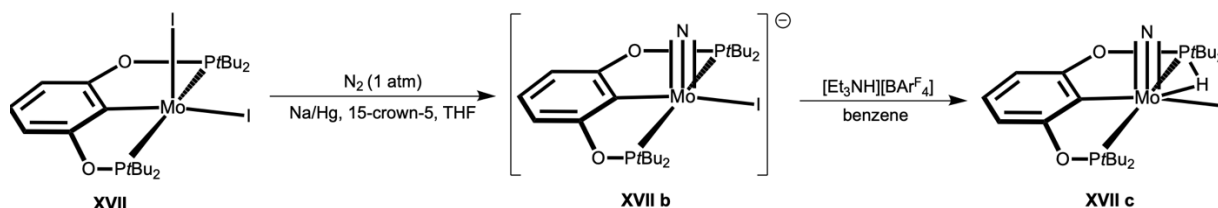


Figure 39 Nitrogen activation with $[Mo(POCOP)I_2]$

In 2018, by using the 1,3-diaminobenzene based *ipso*-chlorinated PCP ligand, the Kirchner group successfully synthesized all group 6 PCP complexes, including the first known PCP-Cr complex, using oxidative addition under solvothermal conditions. In case of Mo and W, the expected diamagnetic seven-coordinate $M(II)$ chloro complexes $[M(PCP^{NEt})(CO)_3Cl]$ (**XVIII**, **XIX**) were isolated. In the case of Cr a mixture of the agostic complex $[Cr(\kappa^3P,CH,P-P(CH)P^{NEt})(CO)_3]$ **XXa** as well as the Cr(III) complex $[Cr(PCP^{NEt})(MeCN)Cl_2]$ **XXb** was obtained.⁶⁸

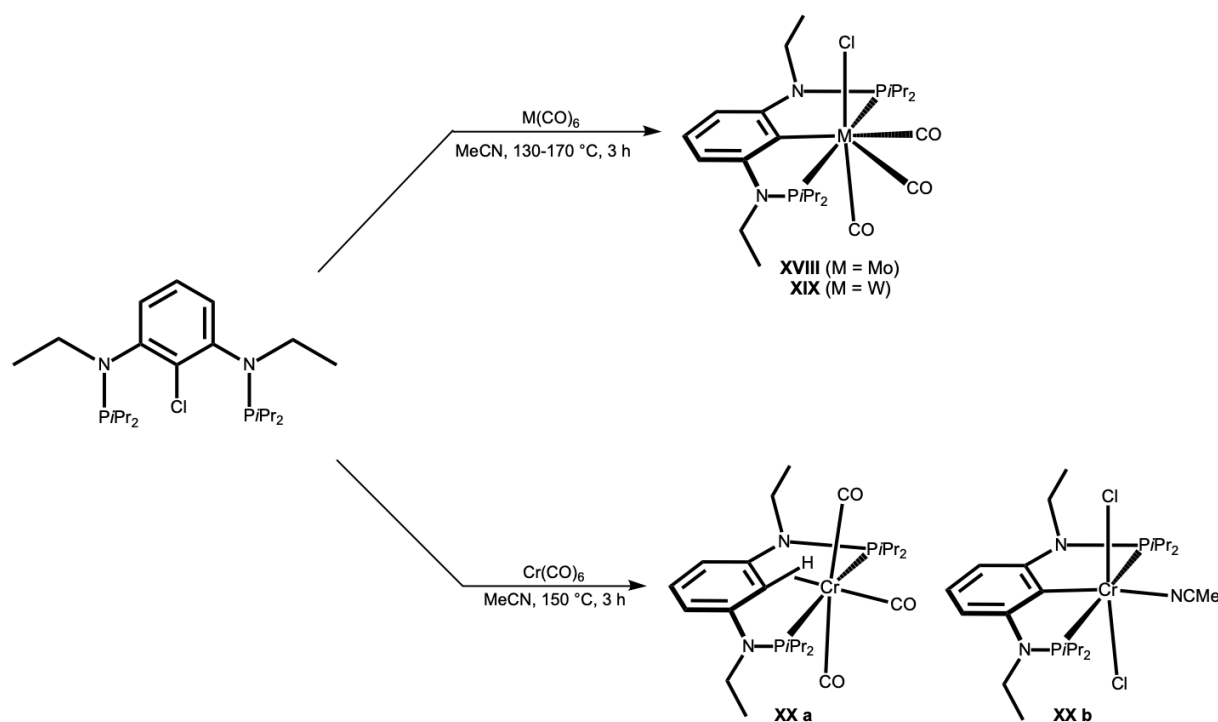


Figure 40 Synthesis of group 6 PCP pincer complexes

Complexes **XVIII** and **XIX** were treated with KC_8 in THF and stirred for two days at room temperature affording the octahedral, diamagnetic and anionic $\text{M}(0)$ complexes $[\text{M}(\text{PCP}^{\text{NEt}})(\text{CO})_3]^-$ **XVIIIa** and **XIXa**.

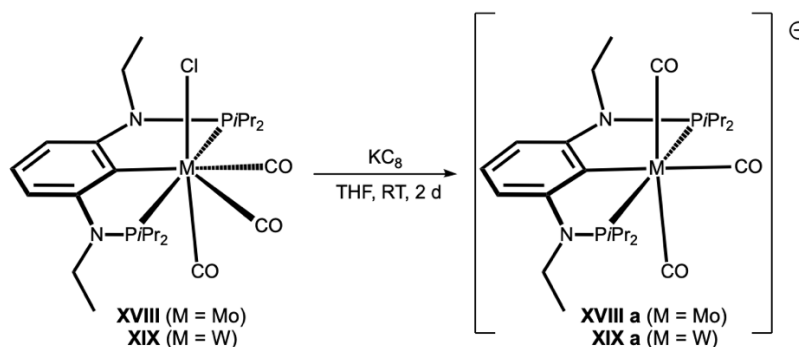


Figure 41 Reduction of the $[\text{M}(\text{PCP}^{\text{NEt}})(\text{CO})_3\text{Cl}]$ complexes

Interestingly, treating **XVIIIa** and **XIXa** with acid afforded for molybdenum the agostic complex $[\text{Mo}(\kappa^3\text{P,CH,P-P}(\text{CH})\text{P}^{\text{NEt}})(\text{CO})_3]$ (see complex **XV**), while tungsten gave the hydride complex $[\text{W}(\text{PCP}^{\text{NEt}})(\text{CO})_3\text{H}]$ (see complex **XVI**)

1.4.6. Complexation Methods for PCP Pincer Complexes

Due to the great stability of the C-H bond of the *ipso*-carbon, the key step in the formation of PCP pincer complexes is the creation of a σ -carbon-metal bond. Cleavage of the bond can either be achieved via direct C-H activation of the metal or by means of oxidative addition of ligand on a low valent metal center. The third possibility of creating a σ -C-M bond is the transmetalation of an *ipso*-lithiated ligand salt with a metal precursor.⁶⁹

1.4.6.1. Direct C-H activation

Direct C-H activation is the most common method for creating the σ -C-M bond, having the advantage of not needing any pre-functionalization of the PCP pincer ligand. The method is dependent upon the metal precursor itself as well as the electronic and steric properties of the phosphine donors of the ligand. Higher temperatures and longer reaction times improve yields of the C-H activation. For this reaction, usually, noble metals in higher oxidation states are used, e.g. PdCl_2 , $\text{Pt}(\text{COD})\text{Cl}_2$ or IrCl_3 . Nickel is the only metal of the first transition row, where direct C-H activation is possible.⁶

The metal does not change its oxidation state during the reaction and the hydrogen of the *ipso*-bond is eliminated as the respective hydrogen halide. Thus, addition of weak base can also increase the efficacy of the reaction, necessitating shorter reaction times. The influence of the electron donors on the reaction conditions was first shown by Venanzi. After exchanging the bulky and electron-releasing *t*-Butyl substituted phosphine donors, with the sterically less demanding but weakly electron withdrawing Phenyl substituted phosphines, milder reaction temperatures could be used to obtain the PCP-pincer complexes in high yield.⁷⁰

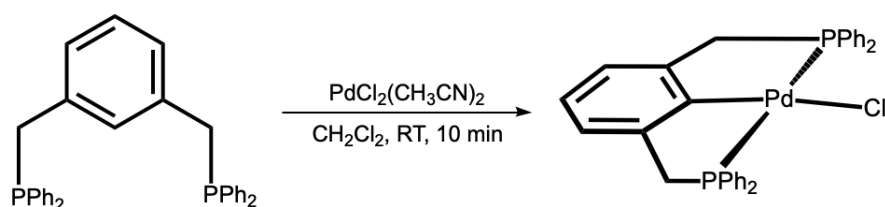


Figure 42 Synthesis of PCP-Pd complexes by Venanzi

Van Koten reported in 1998 the reaction of an NCN pincer ligand with group 10 metals. Instead of the desired cyclometalated pincers, he obtained binuclear complexes. This behavior was attributed to the weaker donating amine electron donors, that are not able to enforce the tridentate coordination geometry needed to create a pincer.⁷¹

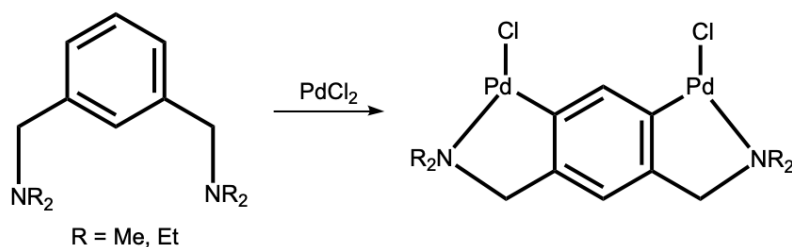


Figure 43 Synthesis of binuclear NC complexes by van Koten

The desired pincer compound was obtained, after introduction of a directing group on the *ipso*-carbon.

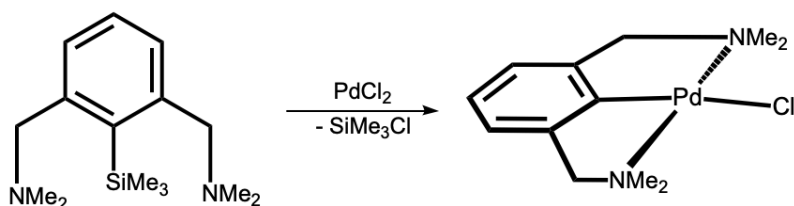


Figure 44 Synthesis of NCN-Pd pincer complex

1.4.6.2. Oxidative Addition

Another way of forming σ -C-M bonds in PCP-complexes is by means of oxidative additions reactions. In a first step, the σ -bonding orbital of the *ipso*-C-H bond donates electron density to a vacant metal-based orbital, thereby creating an agostic bond. In a second step, a populated orbital on the metal center donates electron density to a antibonding σ^* -orbital of the C-H bond. If the backdonation is significant enough, the bond is cleaved, and a PCP-hydride complex is formed.⁷² This reaction increases the oxidation state of the metal by two. High pressure and high temperature favor the reaction, as the initial C-H activation is facilitated.



Figure 45 Mechanism of oxidative addition reactions

The agostic bond can therefore be described as an interaction between an electrophilic metal center and the *ipso* C-H bond. It formally constitutes a three-center two-electron bond. When the agostic transition state is thermodynamically more stable than the fully cleaved hydride complex, the reaction does not progress beyond that step.

When Milstein attempted to prepare Rh(III) PCP pincer complexes via oxidative addition to the cationic Rh(I) complex $[\text{Rh}(\text{C}_2\text{H}_4)(\text{CO})(\text{solv})_n]^+$ ($n = 1, 2$), he observed the formation of the agostic Rh(I) complex $[\text{Cr}(\kappa^3\text{P}, \text{CH}, \text{P}-\text{P}(\text{CH})\text{P})(\text{CO})]^+$. Treatment with the weak base TEA, afforded the neutral Rh(I) complex $[\text{Rh}(\text{PCP})(\text{CO})]$. This

showed that the hydrogen of this agostic bond is acidic and can be abstracted by base. The reaction was reversible via protonation with acid.⁷³

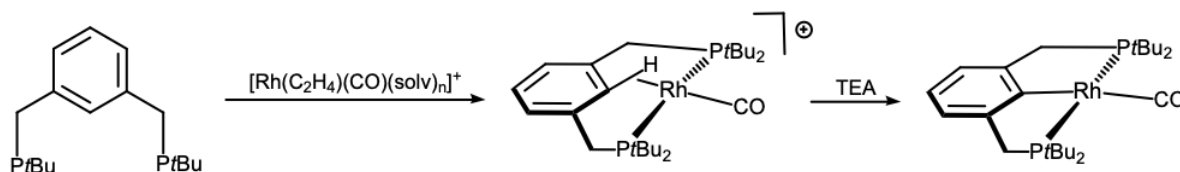


Figure 46 Deprotonation of an agostic complex

Heinekey prepared the analogous neutral Rh(I) complex $[\text{Rh}(\text{POCOP})(\text{CO})]$, utilizing a phosphinite ligand and showed, after protonation, that the agostic Rh(I) complex and the cleaved Rh(III)-hydride complex existed in equilibrium in solution.⁷⁴

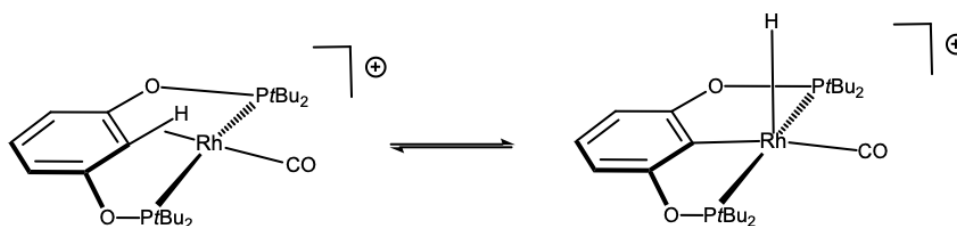


Figure 47 Equilibrium between an agostic and a hydride complex

It was also shown, that not all agostic complexes were convertible to full pincer complexes using base. Treatment of group 6 complexes **XIV** and **XV** even with strong base, like *n*-BuLi and KO*t*Bu, did not lead to deprotonation of the agostic C-H bond.¹¹ The utilization of *ipso*-halogenated PCP ligands, permitted to circumvent these agostic intermediates making it possible to gain access to new base metal pincer complexes using oxidative addition reactions.

1.4.6.3. Transmetalation

The third method of creating a σ -C-M bond is transmetalation. For this reaction the ligand has to be deprotonated at the *ipso*-position with strong base, in most cases *n*-BuLi, creating a ligand salt. This ligand salt is in a next step reacted with a metal precursor, creating a σ -C-M bond with elimination of a lithium salt. However, due to the low acidity of aromatic C-H bonds, lithiation of the *ipso*-position of a PC(H)P ligand is in most cases impossible. However, when substituting the *ipso* hydrogen atom with a

halogen, the lithium species can be obtained in quantitative yield via halogen-metal exchange reactions.⁶⁹

An example of the creation of a PCP complex by using transmetalation is seen in Figure 48. Heinekey prepared the square pyramidal complex [Co(POCOP)I] by first creating the *ipso*-lithiated species with *n*-BuLi and subsequent transmetalation with CoI₂·THF. LiI was eliminated during the reaction.⁷⁵

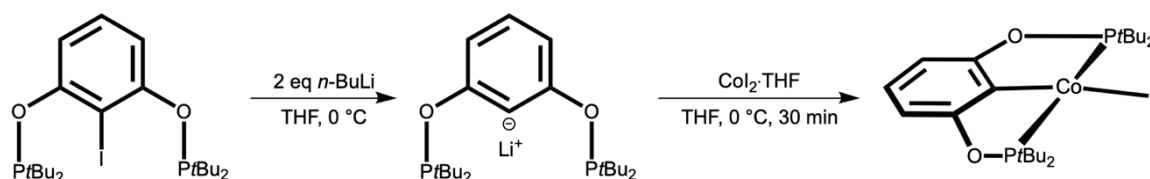
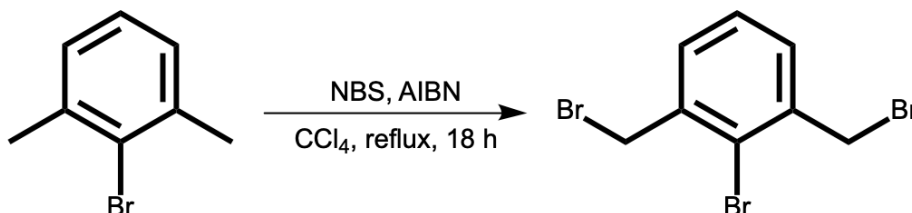


Figure 48 Synthesis of a POCOP-Co complex by mean of transmetallation

2. Experimental Part

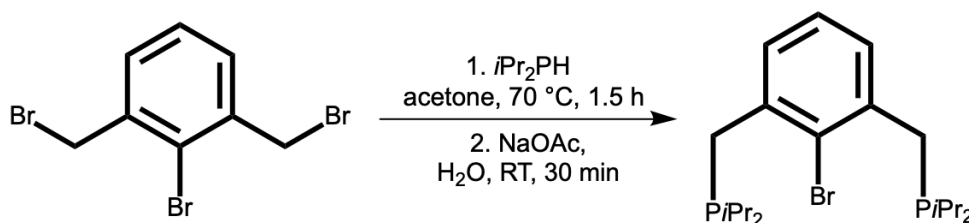
2.1. Synthesis of the Ligand

2-Bromo-1,3-bis(bromomethyl)benzene (**1**)



10 g (54 mmol) 2-bromo-1,3-dimethylbenzene and 19.2 g (108 mmol) *n*-bromosuccinimide were suspended in 80 ml CCl₄ in a one neck flask. 20 mg azobisisobutyronitrile (AIBN) were added and the suspension was refluxed under stirring for 2 h. Thereafter another 20 mg of AIBN was added and the suspension was refluxed for 18 h. The suspension was cooled to room temperature and filtered over silica gel, yielding a clear solution. The solvent was evaporated under reduced pressure, yielding an off-white solid. The crude product was recrystallized from *n*-hexane giving **1** as colorless needles. (10.2 g, 55 %)

¹H NMR (250 MHz, CDCl₃, δ, 20 °C): 7.42 (d, *J* = 7.9 Hz, 2H, CH^{4,6}), 7.29 (t, *J* = 8 Hz, 1H, CH⁵), 4.64 (s, 4H, -CH₂Br). ¹³C{¹H} NMR (63 MHz, δ, CDCl₃, 20 °C) 138.5 (s, C^{1,3}), 131.4 (s, C^{4,6}), 128.0 (s, C⁵), 126.6 (s, C²), 33.8 (s, -CH₂Br).

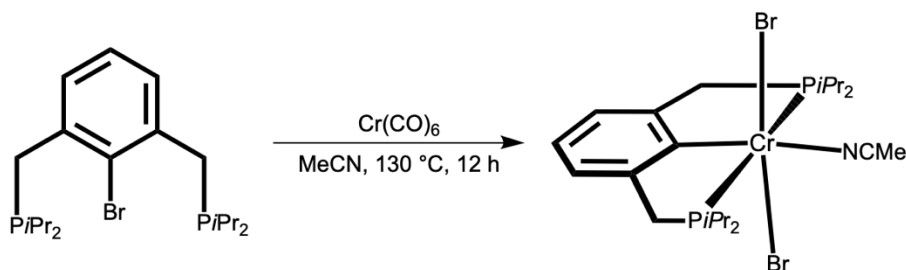
(2-Bromo-1,3-phenylene)bis(methylene))bis(diisopropylphosphane) (**2**)

1.52 g **1** (4.43 mmol) and 1.36 g (11.52 mmol) diisopropylphosphine were dissolved in 8 ml acetone under argon and sealed in a microwave reaction vial. The solution was heated at 70 °C for 90 min and the solution, as well as the formed precipitate, were transferred into a Schlenk tube. The volatiles were removed under reduced pressure and the off-white solid was washed with Et₂O to remove unreacted educt. The diphosponium salt was then dissolved in 15 ml degassed water and subsequently treated with aqueous NaOAc solution (5g (60 mmol) NaOAc in 15 ml degassed water) precipitating the diphosphine. The reaction was stirred for 30 minutes and then the aqueous layer was extracted three times with 40 ml Et₂O. The etheric layer was dried over Na₂SO₄ and after filtration all volatiles were removed in vacuo. The residue was taken up in 40 ml n-pentane and filtered over silica gel. After evaporation of the solvent, **2** was obtained as yellow oil, (900 mg, 49%) and used without further purification.

¹H NMR (400 MHz, C₆D₆, δ, 20 °C): 7.26 (d, J = 7.54 Hz, 2 H, CH^{4,6}), 6.94 (t, J = 7.58 Hz, 1 H, CH⁵), 2.96 (d, J_{HP} = 1.58 Hz, 4H -CH₂P-), 1.67 (dsp, J = 7.11 Hz, J = 1.47 Hz, 4H, -PCH(CH₃)₂), 1.02 (m, 24H, -PCH(CH₃)₂). ¹³C{¹H} NMR (101 MHz, δ, C₆D₆, 20 °C) 141.1 (d, J_{CP} = 8.46 Hz, C^{1,3}), 129.3 (dd, J_{CP} = 11.09 Hz, J_{CP} = 2.25 Hz, C^{4,6}), 126.1 (s, C⁵), 31.4 (d, J_{CP} = 22.91 Hz, -CH₂P-), 24.0 (d, J_{CP} = 16.60 Hz, -PCH(CH₃)₂), 19.7 (dd, J_{CP} = 31.74 Hz, J_{CP} = 13.10 Hz, PCH(CH₃)₂). Ipso C not detected ³¹P{¹H} NMR (162 MHz, δ, C₆D₆, 20 °C) 9.5 (s)

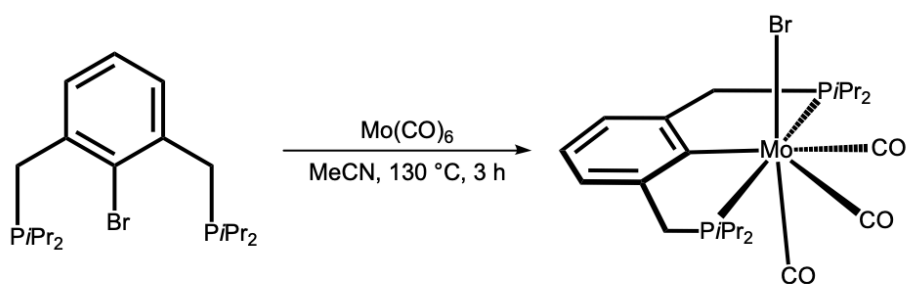
2.2. Synthesis of Complexes

[Cr(PCP)(MeCN)Br₂] (**3**)



100 mg **2** and 53 mg Cr(CO)_6 , suspended in 2.5 ml acetonitrile, were sealed in a microwave tube and heated at 130 °C for 12 h, affording a yellow-red solution. After evaporation of the solvent the remaining solid was washed three times with 10 ml *n*-pentane. The residue was taken up in 3 ml dichloromethane and precipitated with 10 ml *n*-pentane, giving **3** as reddish-brown solid. (45 mg, 40 %) $\mu_{\text{eff}} = 3.7$ (**3**) μ_{B} (Evans method, CH_2Cl_2)

[Mo(PCP)(CO)₃Br] (**4**)

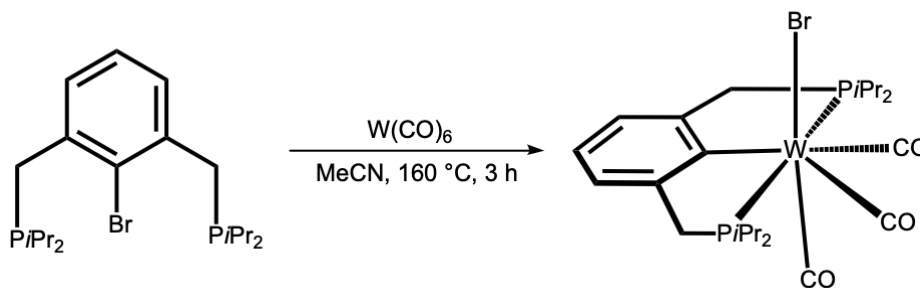


100 mg **2** (0.24 mmol) and 63.2 mg Mo(CO)_6 (0.24 mmol), suspended in 2.5 ml acetonitrile, were sealed under argon in a microwave reaction vial. The vial was heated at 130 °C for 3 h affording a red-brown solution. After cooling to room temperature orange-brown crystals precipitated from the mother liquor. The supernatant solution

was decanted and the crystals were washed twice with 1 ml MeOH to yield **4** (115 mg, 80 %) as orange crystals.

^1H NMR (400 MHz, CD_2Cl_2 , δ , 20 °C): 7.13 (d, J = 7.43 Hz, 2H, $\text{CH}^{4,6}$), 6.99 (t, J = 7.42 Hz, 1H, CH^5), 4.04 (dt, J = 15.47 Hz, J = 4.95 Hz, 2H, $-\text{CH}_2\text{P}-$), 3.72 (dt, J = 15.48 Hz, J = 3.94 Hz, 2H, $-\text{CH}_2\text{P}-$), 2.91 (m, 2H, $-\text{PCH}(\text{CH}_3)_2$), 2.47 (m, 2H, $-\text{PCH}(\text{CH}_3)_2$), 1.32 (m, 18H, $-\text{PCH}(\text{CH}_3)_2$), 1.10 (m, 6H, $-\text{PCH}(\text{CH}_3)_2$). $^{13}\text{C}\{^1\text{H}\}$ NMR (101 MHz, δ , CD_2Cl_2 , 20 °C) 238.1 (br, CO), 224.5 (t, J = 11.98 Hz, CO), 171.3 (t, J = 8.02 Hz, ipso C), 149.1 (t, J = 7.76 Hz, $\text{C}^{1,3}$), 127.4 (s, C^5), 123.1 (t, J = 7.99 Hz $\text{C}^{4,6}$), 40.6 (vt, $-\text{CH}_2\text{P}-$), 27.6 (t, J = 9.52 Hz $-\text{PCH}(\text{CH}_3)_2$), 27.2 (t, J = 10.42 Hz, $-\text{PCH}(\text{CH}_3)_2$), 19.7 (m, $\text{PCH}(\text{CH}_3)_2$). $^{31}\text{P}\{^1\text{H}\}$ NMR (162 MHz, δ , CD_2Cl_2 , 20 °C) 75.1 (s). IR (ATR, ν_{CO} , cm^{-1}) 2008, 1923, 1871. HRMS (ESI^+ , $\text{CH}_3\text{CN}/\text{MeOH}$ + 1% H_2O): m/z calcd for $\text{C}_{23}\text{H}_{35}\text{O}_3\text{BrNaMoP}_2$ $[\text{M}+\text{Na}]^+$ 621.0197 found 621.0181.

$[\text{W}(\text{PCP})(\text{CO})_3\text{Br}]$ (**5**)

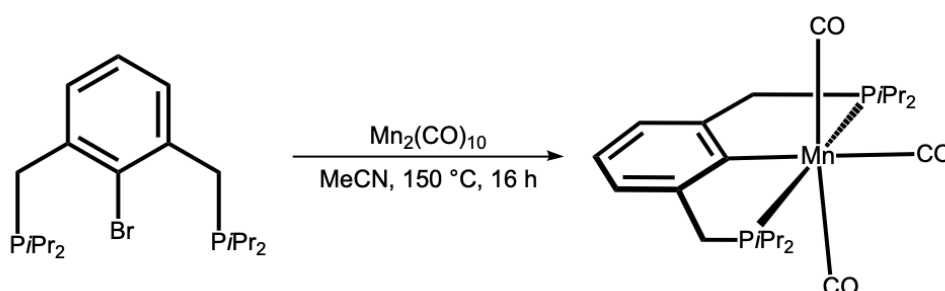


100 mg **2** (0.24 mmol) and 84.4 mg $\text{W}(\text{CO})_6$ (0.24 mmol) were suspended in 2.5 ml acetonitrile and sealed in a microwave reaction vial under argon. The suspension was heated at 160 °C for 3 h affording a dark-brown solution. After cooling to room temperature brown crystals precipitated from the mother liquor. The crystals were separated from the supernatant solution and washed twice with 1 ml methanol. 136 mg **5** (83 %) as yellowish-brown crystals was obtained.

^1H NMR (400 MHz, CD_2Cl_2 , δ , 20 °C): 7.16 (d, J = 7.46 Hz, 2H, $\text{CH}^{4,6}$), 7.02 (t, J = 7.45 Hz, 1H, CH^5), 4.10 (dt, J = 15.63 Hz, J = 4.78 Hz, 2H, $-\text{CH}_2\text{P}-$), 3.74 (dt, 2H, $-\text{CH}_2\text{P}-$), 2.95 (m, 2H, $-\text{PCH}(\text{CH}_3)_2$), 2.51 (m, 2H, $-\text{PCH}(\text{CH}_3)_2$), 1.31 (m, 18H, $-\text{PCH}(\text{CH}_3)_2$),

1.11 (m, 6H, -PCH(CH₃)₂). ¹³C{¹H} NMR (101 MHz, δ, CD₂Cl₂, 20 °C) 232.2 (br, CO), 217.5 (t, J= 9.15 Hz, CO), 168.9 (t, J= 6.80 Hz, ipso C), 150.7 (t, J= 7.74 Hz, C^{1,3}), 127.6 (s, C⁵), 123.1 (t, J= 7.42 Hz, C^{4,6}), 40.8 (vt, -CH₂P-), 27.8 (vt, -PCH(CH₃)₂), 26.8 (vt, -PCH(CH₃)₂), 19.8 (m, PCH(CH₃)₂). ³¹P{¹H} NMR (162 MHz, δ, CD₂Cl₂, 20 °C) 53.6 (s). IR (ATR, ν_{CO}, cm⁻¹) 2000, 1913, 1859. HRMS (ESI⁺, CH₃CN/MeOH + 1% H₂O): *m/z* calcd for C₂₃H₃₅O₃BrNaP₂W [M+Na]⁺ 707.0652 found 707.0620.

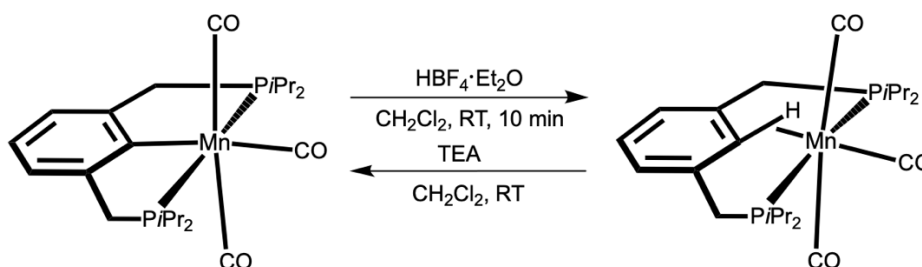
[Mn(PCP)(CO)₃] (**6**)



100 mg **2** (0.24 mmol) and 46.8 mg Mn₂(CO)₁₀ (0.12 mmol) were heated in MeCN at 150 °C for 16 h in a microwave reaction vial, yielding a clear orange solution. After evaporation of the solvent the crude orange product was purified by column chromatography (*n*-hexane:EtOAc 10:3) and the off-white residue was recrystallized from a concentrated solution in *n*-hexane:EtOAc (10:1) at -30 °C to yield 35 mg **6** (31 %) as off-white crystals.

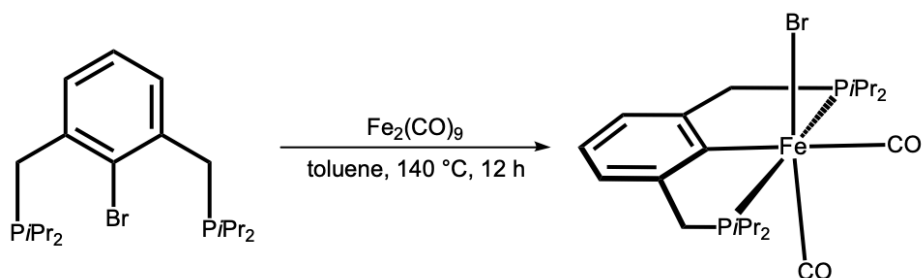
¹H NMR (400 MHz, CD₂Cl₂, δ, 20 °C): 6.99 (d, J= 7.39 Hz, 2H, CH^{4,6}), 6.80 (t, J= 7.43 Hz, 1H, CH⁵), 3.36 (d, J= 7.33 Hz, 4H, -CH₂P-), 2.37 (m, 4H, -PCH(CH₃)₂), 1.28 (dd, J= 13.32 Hz, J= 7.04 Hz, 12H, -PCH(CH₃)₂), 1.22 (dd, 12H, J= 13.27 Hz, J= 7.18 Hz, -PCH(CH₃)₂). ¹³C{¹H} NMR (101 MHz, δ, CD₂Cl₂, 20 °C) 226.7 (br, CO), 223.7 (t, J= 23.24 Hz, CO), 173.0 (t, J= 8.23 Hz, ipso C), 148.8 (t, J= 9.06 Hz, C^{1,3}), 123.7 (s, C⁵), 121.9 (t, J= 6.76 Hz, C^{4,6}), 41.2 (t, J= 10.03 Hz, -CH₂P-), 41.0 (t, J= 10.00 Hz, -CH₂P-) 28.2 (m, -PCH(CH₃)₂), 26.8 (vt, -PCH(CH₃)₂), 19.4 (d, J = 18.07 Hz, PCH(CH₃)₂). ³¹P{¹H} NMR (162 MHz, δ, CD₂Cl₂, 20 °C) 100.3 (s). IR (ATR, ν_{CO}, cm⁻¹) 1985, 1892, 1873. HRMS (ESI⁺, CH₃CN/MeOH + 1% H₂O): *m/z* calcd for C₂₃H₃₆O₃MnP₂ [M+H]⁺ 477.1520 found 477.1515.

[Mn(PC(H)P)(CO)₃]BF₄ (**6a**)



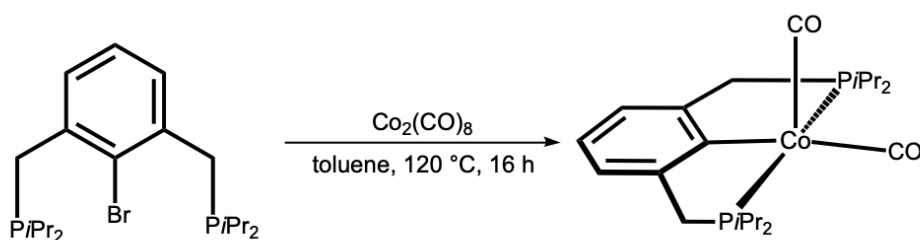
7 mg (14.7 μ mol) **6** were dissolved in 2 ml CH₂Cl₂ and subsequently 2.5 μ l (17.6 μ mol, 1.2 eq) HBF₄·Et₂O were added and stirred for 10 minutes, affording a dark-orange solution. The solvent was evaporated under reduced pressure and the orange-red solid was washed three times with 1 ml n-pentane. To remove the excess of the HBF₄·Et₂O, the residue was taken up in 2 ml CH₂Cl₂ and precipitated with 4 ml n-pentane, twice, yielding **6a** as orange-red solid (6 mg, 86 %). Crystals suitable for X-ray diffraction were obtained by slow evaporation of a concentrated solution of **6a** in CH₂Cl₂. Treating a solution of **6a** in CH₂Cl₂ with an excess of TEA led to an immediate discoloration of the solution. After removing of the solvent, the colorless residue was characterized as **6**, showing the reversibility of the reaction.

¹H NMR (600 MHz, CD₂Cl₂, δ , 20 °C): 7.70 (t, J = 7.62 Hz, 1H, CH⁵), 7.09 (dd, J = 7.30 Hz, J = 2.30 Hz, 2H, CH^{4,6}), 4.05 (s, 1H, CH ipso), 3.55 (m, 2H, -CH₂P-), 3.08 (m, 2H, -CH₂P-), 2.86 (sep, J = 7.16 Hz 2H, -PCH(CH₃)₂), 2.47 (sep, J = 7.42 Hz 2H, -PCH(CH₃)₂), 1.46 (m, 6H, -PCH(CH₃)₂), 1.35 (m, 18H, -PCH(CH₃)₂). ¹³C{¹H} NMR (151 MHz, δ , CD₂Cl₂, 20 °C) 226.0 (br, CO), 216.7 (q, J = 23.24 Hz, CO), 155.6 (s, C^{1,3}), 137.5 (vt, C⁵), 126.7 (vt, J = 5.72 Hz, C^{4,6}), 84.3 (t, J = 6.63 Hz, ipso C), 33.4 (m, -CH₂P-), 29.5 (m, -PCH(CH₃)₂) 26.6 (m, -PCH(CH₃)₂), 19.0 (m, PCH(CH₃)₂). ³¹P{¹H} NMR (243 MHz, δ , CD₂Cl₂, 20 °C) 53.4 (s). IR (ATR, ν_{CO} , cm⁻¹) 2043, 1958, 1911. HRMS (ESI⁺, CH₃CN/MeOH + 1% H₂O): *m/z* calcd for C₂₃H₃₅O₃MnP₂ [M-H]⁺ 477.1442 found 476.1436.

[Fe(PCP)(CO)₂Br] (**7**)

100 mg **2** (0.24 mmol) and 44 mg Fe₂(CO)₉ (0.12 mmol) were heated in Toluene at 140 °C for 16 h in a microwave reaction vial, yielding a clear yellow solution. The solvent was evaporated, and the orange precipitate twice washed with 2 ml *n*-pentane yielding 73 mg **7** (58 %) as orange solid. Crystals suitable for X-ray diffraction were obtained by slow diffusion of *n*-pentane in a concentrated solution of **7** in THF:

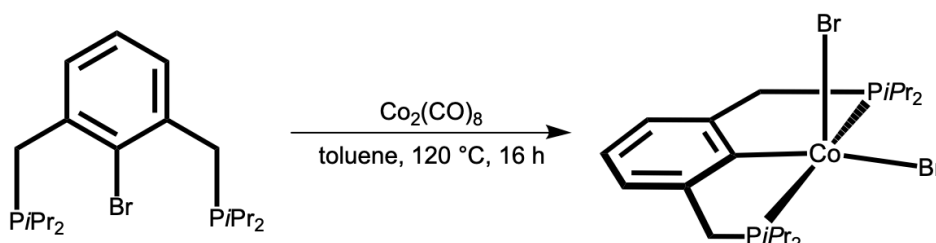
¹H NMR (250 MHz, C₆D₆, δ, 20 °C): 7.24 (s, 3H, CH^{4,5,6}), 3.64 (dt, 2H, -CH₂P-), 3.28 (dt, 2H, -CH₂P-), 3.18 (m, 2H, -PCH(CH₃)₂), 2.10 (m, 2H, -PCH(CH₃)₂), 1.32 (q, J= 7.32 Hz, 6H, -PCH(CH₃)₂), 1.11 (m, 12H, -PCH(CH₃)₂). ¹³C{¹H} NMR (63 MHz, δ, C₆D₆, 20 °C) 148.4 (t, C^{1,3}), 125.3 (s, C⁵), 123.0 (t, J= 7.56 Hz, C^{4,6}), 38.7 (t, J= 14.79 Hz, -CH₂P-), 26.4 (m, -PCH(CH₃)₂), 19.5 (d, J= 25.48 Hz, PCH(CH₃)₂). Carbonyls and ipso-C not detected. ³¹P{¹H} NMR (101 MHz, δ, C₆D₆, 20 °C) 88.2 (s). IR (ATR, ν_{CO}, cm⁻¹) 1993, 1938, HRMS (ESI⁺, CH₃CN/MeOH + 1% H₂O): *m/z* calcd for C₂₂H₃₅O₂FeP₂ [M-Br]⁺ 449.1462 found 449.1456.

[Co(PCP)(CO)₂] (**8a**)

50 mg **2** (0.12 mmol) and 20.5 mg $\text{Co}_2(\text{CO})_8$ (0.06 mmol) were heated in toluene at 120 °C for 16 h in a microwave reaction vial, yielding a green-yellow solution and a green precipitate. The solution was separated from the precipitate and after evaporation of the solvent the residue was extracted with benzene. **8a** was obtained as yellow solid after evaporation of the solvent. (24 mg, 44%)

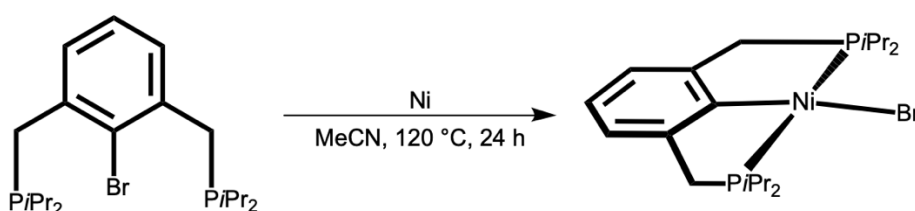
^1H NMR (600 MHz, C_6D_6 , δ , 20 °C): 6.96 (s, 3H, $\text{CH}^{4,5,6}$), 3.03 (vt, ^4H , $-\text{CH}_2\text{P}-$), 1.93 (m, 4H, $-\text{PCH}(\text{CH}_3)_2$), 1.14 (app q, $J = 7.03$ Hz, $J = 7.84$ Hz 12 H, $-\text{PCH}(\text{CH}_3)_2$), 0.96 (app q, 12 H, $J = 7.03$ Hz, $J = 6.56$ Hz, $-\text{PCH}(\text{CH}_3)_2$). $^{13}\text{C}\{^1\text{H}\}$ NMR (151 MHz, δ , C_6D_6 , 20 °C) 210.3 (br, CO), 169.8 (t, $J = 15.80$ Hz, ipso C), 147.2 (t, $J = 11.47$ Hz, $\text{C}^{1,3}$), 123.0 (s, C^5), 121.7 (t, $J = 8.72$ Hz, $\text{C}^{4,6}$), 39.0 (dd, $J = 15.02$ Hz, $J = 12.53$ Hz $-\text{CH}_2\text{P}-$), 27.3 (t, $J = 9.84$ Hz $-\text{PCH}(\text{CH}_3)_2$), 18.7 (d, $J = 18.41$ Hz, $\text{PCH}(\text{CH}_3)_2$). $^{31}\text{P}\{^1\text{H}\}$ NMR (243 MHz, δ , C_6D_6 , 20 °C) 102.9 (s). IR (ATR, ν_{CO} , cm^{-1}) 1966, 1907.

$[\text{Co}(\text{PCP})(\text{CO})_2]$ (**8b**)



8b was analogously prepared as **8a**. The solution was separated from the precipitate and the precipitate washed with benzene (5 ml). **8b** was obtained as green solid. (30 mg, 45%) $\mu_{\text{eff}} = 3.0 \mu_{\text{B}}$ (Evans method, CH_2Cl_2)

$[\text{Ni}(\text{PCP})\text{Br}]$ (**9**)



50 mg (0.12 mmol) **2** and 21 mg (0.36 mmol) nickel metal were suspended in 2 ml acetonitrile and the mixture was heated at 120 °C for 24 h. A green-yellow solution was separated from the excess metal and the solvent was evaporated under reduced pressure. The residue was then extracted with 30 ml *n*-pentane, and after evaporation of all volatiles, **9** was obtained as yellow solid. (43 mg, 75 %)

^1H NMR (250 MHz, CD_2Cl_2 , δ , 20 °C): 6.93 (br, 3H, $\text{CH}^{4,5,6}$), 3.11 (vt, 4H, $-\text{CH}_2\text{P}-$), 2.38 (m, 4H, $-\text{PCH}(\text{CH}_3)_2$), 1.45 (dvt, 12H, $-\text{PCH}(\text{CH}_3)_2$), 1.19 (dvt, 12H, $-\text{PCH}(\text{CH}_3)_2$). $^{31}\text{P}\{^1\text{H}\}$ NMR (101 MHz, CD_2Cl_2 , δ , 20 °C): 61.1. Chemical shifts consistent with literature data.

3. Results and Discussion

3.1. Ligand design and synthesis

The 1,3-diaminobenzene-based systems used by the Kirchner group proved to be effective in the complexation reactions with the group 10 metals as well as cobalt. However, attempts to create cyclometalated compounds with other base metals failed, as the C-H bond could not be activated sufficiently, even in the presence of strong bases. By utilizing oxidative addition reactions under solvothermal conditions only the PCP-W complex was obtained, chromium and molybdenum merely formed the agostic compounds.

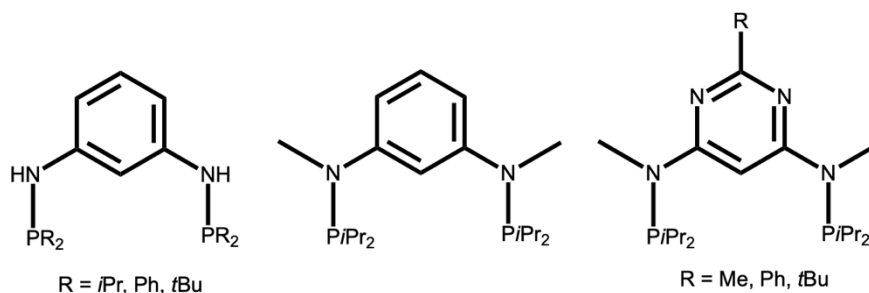


Figure 49 PCP ligands used by the Kirchner group

In an attempt to increase the acidity of the *ipso* C-H bond, a pyrimidine-based ligand was introduced in 2016. However, due to the directing effect of the pyrimidine nitrogen atoms, it was not possible to use *n*-BuLi for the CH activation, limiting its scope to Ni-complexes. When used in oxidative addition reactions, inadvertently, metal PN complexes were formed instead of the desired PCP complexes, when using Me and Ph as para substituents of the ring. By blocking the nitrogen atoms of the ring with the bulky *t*Bu substituent, it was indeed possible to synthesize the analogous PCP-W complex, while for Mo a mixture between the cleaved hydride complex and the agostic complex was obtained.¹³

In a next step with the aim of facile activation of the *ipso*-carbon bond, as well as for potential use in transmetalation reactions a new class of ligands bearing *ipso*-halogenated benzene-backbones, was planned. To investigate potential differences in

reactivity caused by the linking groups, ligands with O, NEt and CH₂ linkers were synthesized.

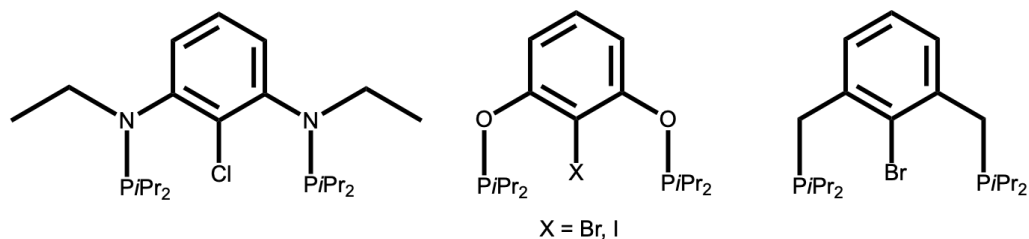


Figure 50 New class of PCP pincer ligands

To synthesize ligand **2**, the precursor 2-bromo-1,3-dimethylbenzene was first converted to the 2-bromo- α,α' -dibromo-*m*-xylene **1** by using the Wohl-Ziegler bromination. As a radical starter AIBN was used. To increase the yield, the radical starter was added in batches to the reaction mixture. As the final purification of **2** proved to be very difficult, it was paramount to only use highly pure educts. Therefore, the raw product was carefully recrystallized from *n*-hexane, yielding colorless white needles.

In a next step **1** was to be reacted with (*i*Pr)₂PH, creating the quaternary di-phosphonium salt, which in presence of a base can be deprotonated to the ligand **2**. However, heating a solution of **1** with the phosphine and TEA in THF, did not yield **2**, as suggested in literature.⁷⁶ Reaction control using ³¹P{¹H} NMR only showed yields of about 3 %, and mostly unreacted dialkyl-phosphine. This can probably be attributed to **1** forming of a quaternary amine with TEA, which prohibits any further reaction.

Instead, another synthesis route for **2** was chosen, where the dialkyl-phosphine was reacted with **1** to yield the insoluble di-phosphonium salt which was then isolated. The compound is air stable, but hygroscopic. This salt can subsequently be deprotonated in aqueous solution and the ligand is then extracted with diethyl ether.⁷⁷ The ligand was obtained in yield of about 50 % as yellow oil, with NMR spectroscopy showing it to be sufficiently pure. **2** rapidly oxidizes in air, small phosphine oxide impurities, however, can be removed by filtration over silica gel.

3.2. Complex synthesis

In analogy to the work of Himmelbauer where the *ipso*-halogenated N-linked PCP ligand was used,⁶⁸ **2** was reacted with group 6 hexacarbonyl complexes under solvothermal conditions at temperatures of 130 – 160 °C with reaction times of 3 – 12 h.

With Cr(CO)₆ a mixture of products was obtained. In analogy to the reaction of the N-linked PCP ligand, a yellow solid was extracted from the reaction mixture with *n*-pentane, and a very air sensitive residual burgundy red solid, that showed good solubility in THF and CH₂Cl₂, was obtained. Evans NMR measurement of the red solid gave a magnetic moment of $\mu_{\text{eff}} = 3.7 \mu_{\text{B}}$, which is consistent with a d³ species, indicating a oxidation state of Cr(III). The yellow substance was identified as a mixture of diamagnetic species. IR measurement of the yellow substance showed multiple CO bands at around 1800 cm⁻¹, with at least two meridional CO species present. The meridional species were identified via the weaker CO band at higher wave numbers of 1930 – 1960 cm⁻¹, which can be attributed to the symmetrical stretch of all three CO ligands. Therefore, in analogy to the reaction with the N-linked PCP complex, it is reasonable, to conclude that an agostic Cr(0) and various similar side-products are formed in this reaction. As of yet, no single crystals of the burgundy Cr(III) compound were obtained, however it can be assumed that this compound is indeed the desired pincer [Cr(PCP)(MeCN)Br₂] (**3**).

The reaction of Mo(CO)₆ with the ligand afforded a reddish-brown solution. While the reaction vial was cooled to room temperature, crystals precipitated from the supernatant solution. These orange crystals were washed with MeOH and proved to be suitable for X-ray diffraction.

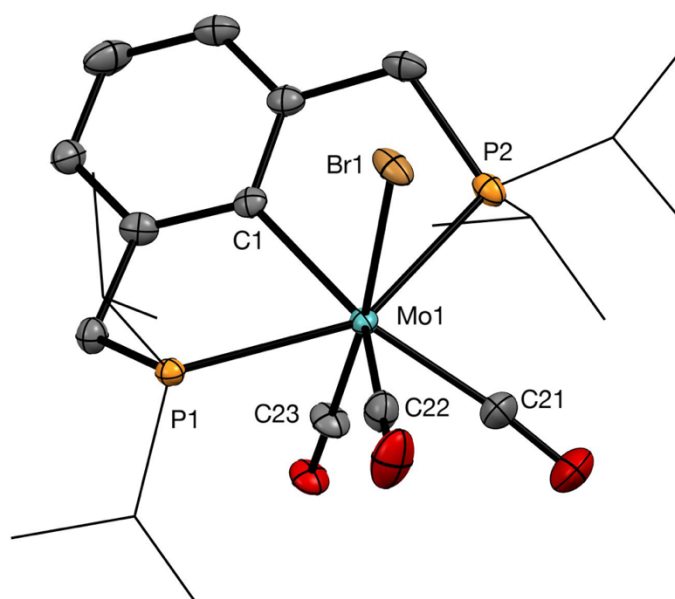


Figure 51 Crystal Structure of $[\text{Mo}(\text{PCP})(\text{CO})_3\text{Br}]$ (**4**) with 50 % thermal ellipsoids. H omitted for clarity. Selected bond lengths (Å) and bond angles (°): Mo1-C1 2.286(4), Mo1-C21 1.987(6), Mo1-C22 2.023(6), Mo1-C23 1.952(8), Mo1-Br1 2.697(1), Mo1-P1 2.524(1), Mo1-P2 2.523(1), P1-Mo1-P2 147.84(4), C1-Mo1-C21 141.98, Br1-Mo1-C23 173.13.

Complex **4** shows a coordination geometry that can best be described as distorted capped-trigonal-prismatic. C1 is hereby capping the quadrilateral face of the prism. This is in contrast to complex $[\text{Mo}(\text{PCP}^{\text{NEt}})(\text{CO})_3\text{Cl}]$ (**XVIII**) that showed a capped octahedral coordination geometry, with an unusual interaction of a carbonyl moiety with the *ipso*-carbon of the ligand. The bond angle between P1-Mo1-P2 is 147.84°. The bond length of the σ -bond C1-Mo1 is with 2.286 Å longer than the C1-Mo1 length observed in complex **XVIII** (2.227 Å). Figure 51 shows the complex in its most abundant solid phase isomer, as the bromine substituent was observed at every carbonyl position in lower percentages. The abundance of the isomer shown is 57.2 %. The second most abundant isomer, where C23 and Br1 are interchanged has an abundance of 29.4 %.

$^{31}\text{P}\{^1\text{H}\}$ NMR spectroscopy showed a singlet at 75.1 ppm. In the $^{13}\text{C}\{^1\text{H}\}$ NMR spectrum two carbonyl signals were observed as a broad singlet at 238.1 and a triplet at 224.5, that showed a coupling constant of 11.98 Hz. The singlet and the triplet were in an integral ratio of 2:1. DFT calculations made for the similar complexes **XVIII** and **XIX** suggest rapid interchange (pseudorotation) of the two basal carbonyl (C21, C22) ligands, with a coalescence temperature below -50 °C. The exchange of the apical

carbonyl (C23) is slower, which makes it possible to resolve it as a triplet, even at RT. The signal for the *ipso*-carbon was detected as a triplet at 171.3 ppm with a J_{C-P} coupling constant of 8.02 Hz. The complex showed three distinct CO bands in the IR spectrum at 2008, 1923 and 1871 cm^{-1} .

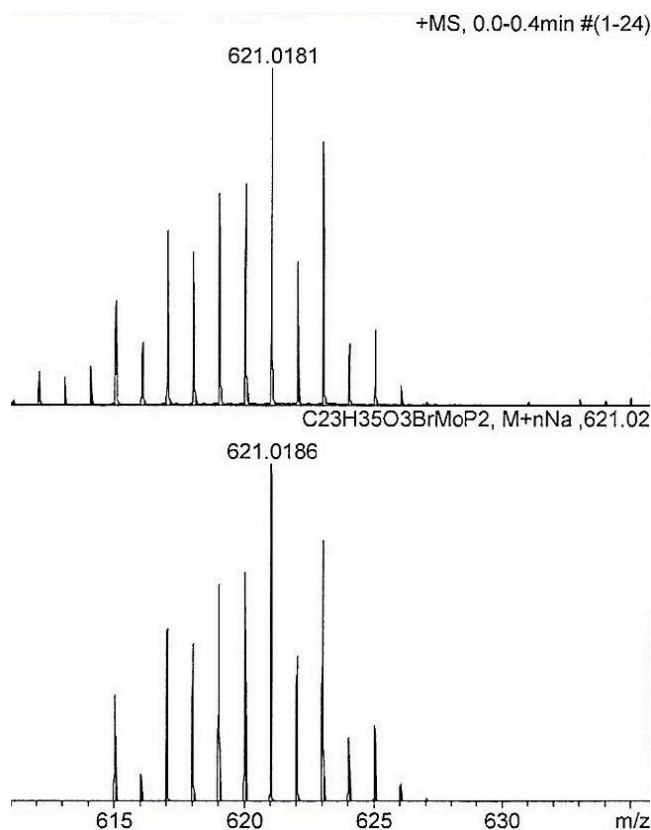


Figure 52 Positive-ion ESI full scan mass spectra of **4**. Mass calculations are based on the lowest mass molybdenum isotope (^{92}Mo) and monoisotopic values.

For complex **4** also a positive ion electrospray ionization high-resolution mass spectroscopy (ESI-HRMS) spectrum was measured. A $[\text{M}+\text{Na}]^+$ peak at 621.0181 m/z was found. Figure 52 shows the isotope pattern of the measurement and below the simulated spectrum.

The reaction of $\text{W}(\text{CO})_6$ and **2** gave a brown solution. After cooling to room temperature, crystals were obtained, that after washing with MeOH also proved suitable for single-crystal X-ray diffraction analysis.

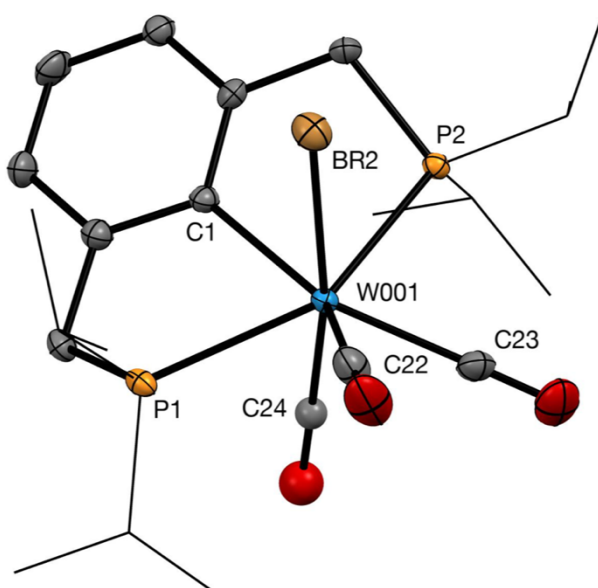


Figure 53 Crystal Structure of $[W(PCP)(CO)_3Br]$ (**5**) with 50 % thermal ellipsoids. H omitted for clarity. Selected bond lengths (Å) and bond angles (°): W001-C1 2.286(1), W001-C23 2.030(3), W001-C22 1.996(5), W001-C24 1.967(4), W001-Br2 2.689(8), W001-P1 2.524(0), W001-P2 2.522(2), P1-W001-P2 148.42, C1-W001-C23 144.48, Br2-W001-C24 170.23.

The structure of **5** was found to be analogous to **4**. It also shows a distorted capped-trigonal-prismatic coordination geometry. Due to nearly identical ionic radii of Mo and W, the distance between the metal center and the *ipso*-carbon is with 2.286 Å practically the same as in **4** and slightly longer than the 2.219 Å observed on the analogous complex $[W(PCP^{NEt})(CO)_3Cl]$ (**XIX**). The P1-W001-P1 bond angle is 148.42°. The tungsten-phosphorus, as well as tungsten-carbonyl bond lengths are also very similar to those seen in **4**.

The $^{31}P\{^1H\}$ NMR spectrum shows a singlet at 53.6 ppm. As tungsten does have an NMR active isotope ^{183}W (14 % abundance, $I = 1/2$), phosphorus-tungsten coupling can be observed, and a doublet is superimposed, as satellite signals, over the dominant singlet with a $^1J_{W-P}$ coupling constant of 84 Hz. In the $^{13}C\{^1H\}$ NMR spectrum of **5**, analogously to complex **4**, a broad singlet at 232.2 and a triplet at 217.5 ppm in a ratio of 2:1 are observed with a coupling constant of 9.15 Hz. The triplet also shows satellite signals due to ^{183}W coupling with a $^1J_{C-W}$ coupling constant of 73 Hz.

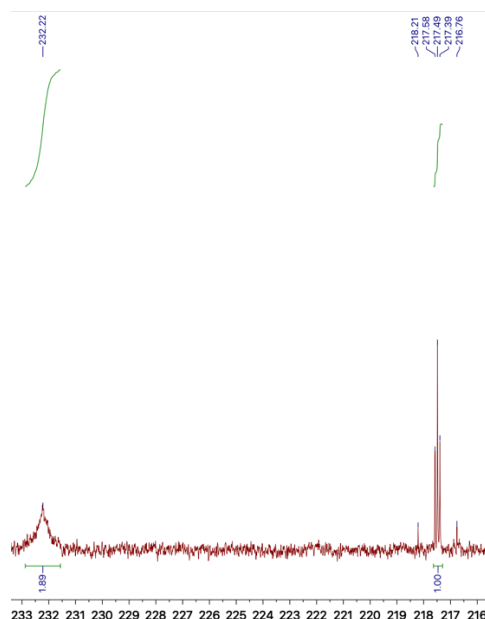


Figure 54 $^{13}\text{C}\{^1\text{H}\}$ NMR Carbonyl signals of **5** in CD_2Cl_2 , triplet shows coupling with ^{183}W

The *ipso*-carbon was detected as a triplet at 168.9 ppm, with a $J_{\text{C-P}}$ coupling constant of 6.80 Hz. In the IR spectrum **5** three distinct carbonyl bands at 2000, 1913 and 1859 cm^{-1} are observed. The positive ion ESI-HRMS spectrum of **5** gave rise to a $[\text{M}+\text{Na}]^+$ peak at 707.0620 m/z. Figure 55 shows the isotope pattern of the measurement and below the simulated spectrum.

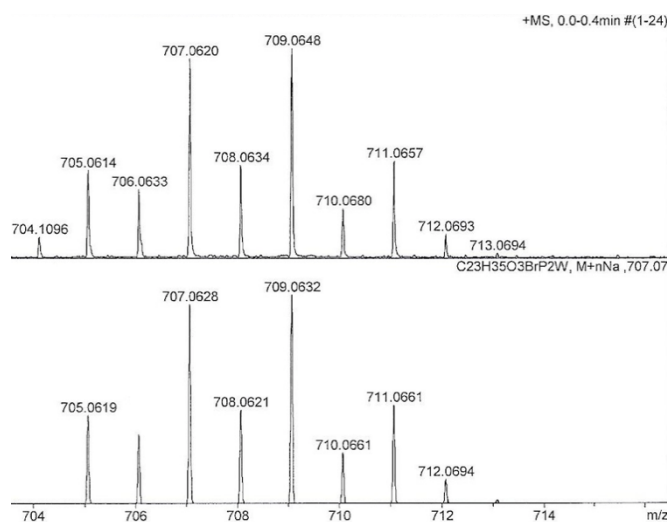


Figure 55 Positive-ion ESI full scan mass spectra of **5**.

In a next step the ligand was reacted with $\text{Mn}_2(\text{CO})_{10}$. After the solvothermal reaction, a clear orange solution was obtained. Reaction control with $^{31}\text{P}\{^1\text{H}\}$ NMR showed a full conversion of the ligand and only one diamagnetic species at 100.8 ppm was

observed. The diamagnetic nature of the product suggested a Mn(I), low spin d^6 complex. In accordance with the work of Himmelbauer,⁶⁸ the orange crude product was purified by means of silica gel column chromatography. Thereby complex **6** proved to be exceptionally stable, as the chromatography was performed in air and a solvent mixture of *n*-hexane/EtOAc 10:3 (technical grade solvents) was used. Complex **6** was afforded as off-white solid in a yield of 40 %. The complex was then taken up in a mixture of *n*-hexane:EtOAc 10:1 and recrystallized at -30 °C, giving macroscopic, transparent, slightly yellow crystals, that were suitable for X-ray diffraction analysis, with a total yield of 31 %.

The low yields and the presence of an orange side product, combined with full consumption of the ligand was seen by $^{31}\text{P}\{^1\text{H}\}$ NMR spectroscopy. This suggests that another, presumably paramagnetic, product was likely formed. A disproportionation reaction to a Mn(I) and Mn(III) species seems likely, however, as yet the latter complex could not be isolated.

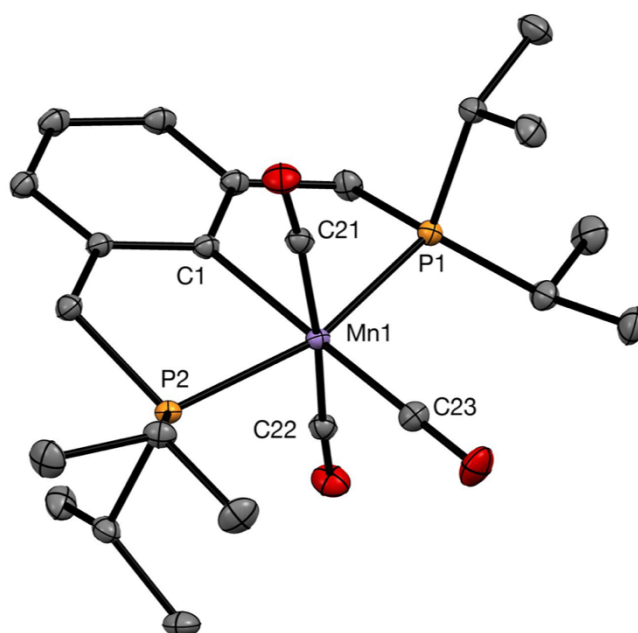


Figure S6 Crystal Structure of $[\text{Mn}(\text{PCP})(\text{CO})_3]$ (**6**) with 50 % thermal ellipsoids. H omitted for clarity.

Selected bond lengths (Å) and bond angles (°): Mn1-C1 2.093(1), Mn1-C23 1.800(1), Mn1-C21 1.822(1), Mn1-C22 1.823(1), Mn1-P1 2.2794(4), Mn1-P2 2.772(4), P1-Mn1-P2 162.331(11), C1-Mn1-C23 178.70(4), C21-Mn1-C22 172.25(4).

The coordination geometry of **6** is a slightly distorted octahedron. Particularly the P1-Mn1-P2 angle of 162.33° differs significantly from the 180° expected in a regular octahedron. The C1-Mn1 bond length is 2.093 \AA , which is slightly longer than the 2.049 \AA bond length observed in the N-linked PCP **XIII**. The P1-Mn1 distance is 2.279 \AA , the P2-Mn1 distance 2.772 \AA . The Mn1-C23 distance (1.800 \AA) of the basal carbonyl ligand is slightly longer than that of the apical carbonyls Mn1-C21(1.822 \AA) and Mn1-C22 (1.823 \AA).

The complex exhibits three distinct CO bands in the ATR-IR spectrum at 1873 , 1892 and 1985 cm^{-1} , specific for the meridional geometry of the carbonyls. $^{31}\text{P}\{^1\text{H}\}$ NMR spectroscopy displays a singlet at 100.3 ppm . The carbonyl signals appear in the $^{13}\text{C}\{^1\text{H}\}$ NMR spectrum as broad singlet and triplet at 226.7 and 223.7 ppm , with an integral ratio of 1:2, respectively. The $J_{\text{C-P}}$ coupling constant of the triplet, assigned to the apical carbonyls was measured as 23.24 Hz . The *ipso*-carbon was found as a triplet at 173.0 ppm , with a $J_{\text{C-P}}$ coupling constant of 8.23 Hz .

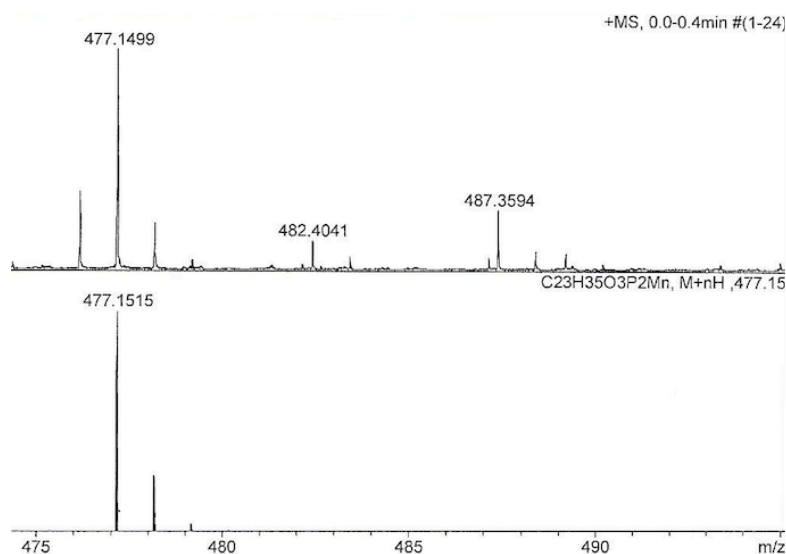


Figure 57 Positive-ion ESI full scan mass spectra of **6**.

Figure 57 shows the isotope pattern of **6** in the positive ion ESI-HRMS spectrum. The complex was found as $[\text{M}+\text{H}]^+$. The measured spectrum is seen at the top, the simulation on the bottom.

By protonation of **6** with $\text{HBF}_4 \cdot \text{Et}_2\text{O}$ the cationic agostic Mn(I) complex **6a** was obtained.

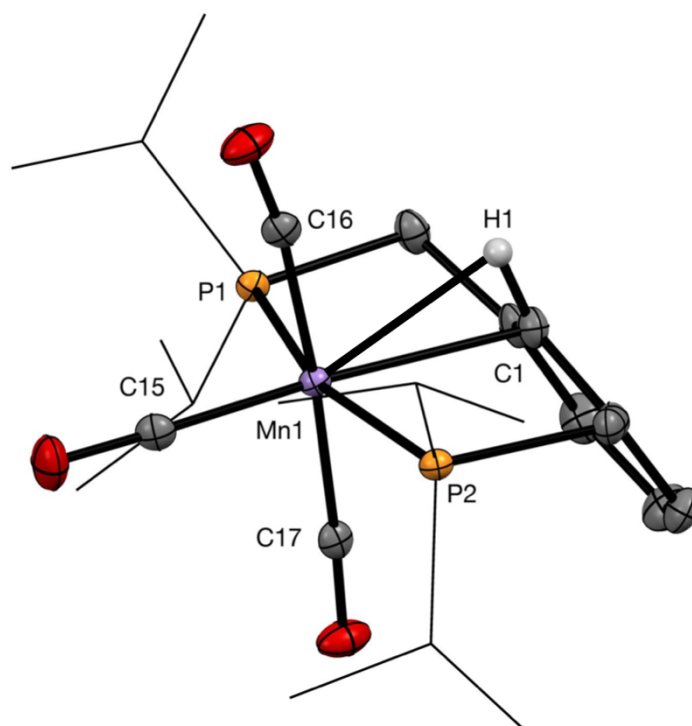


Figure S8 Crystal Structure of $[\text{Mn}(\text{PC}(\text{H})\text{P})(\text{CO})_3]$ (**6a**) with 50 % thermal ellipsoids. H and counterion omitted for clarity. Selected bond lengths (Å) and bond angles (°): Mn1-C15 1.767(3), Mn1-C16 1.851(3), Mn1-C17 1.846(3), Mn1-C1 2.408(3), Mn1-P1 2.3331(8), Mn1-P2 2.3334(9), Mn1-H1 2.29(3), C1-H1 0.96(3), P1-Mn1-P2 163.96(4), C16-Mn1-C17 174.73(12), C1-Mn1-C15 175.33(12).

The complex features a distorted octahedral geometry, where especially the P1-Mn1-P2 bonding angle of 163.96° differs significantly from the 180° expected in an octahedron. The three carbonyl ligands as well as the agostic $\eta^2\text{-C}_{\text{aryl}}\text{-H}$ bond define the equatorial plane, while the phosphine moieties set up the axial positions. The C1-Mn1 bond is with 2.408 Å extremely long. For comparison the Mn-C bond in **6** is 2.093 Å. The bond length is even unusually long compared the related agostic complex $[\text{Mn}(\text{PC}(\text{H})\text{P}^{\text{NEt}})(\text{CO})_3]\text{BF}_4$ (**XIIlb**) where it was measured as 2.249 Å. The hydrogen of the agostic bond (H1) also features an interaction with the metal center, with an observed bond length of 2.29 Å. This interaction can also be observed in the ^1H NMR spectrum, where the signal of the proton attached to the *ipso*-carbon is slightly shifted to the high field to 4.05 ppm. In comparison, the Mn-H1 distance of **XIIlb** is lower, measured at 1.993 Å, indicating a stronger H-Mn interaction than in **6a**; a conclusion

that can also be deduced based on the greater high-field shift in the ^1H NMR spectrum of **XIIIb**, where it was observed at 1.36 ppm.

The hydrogen of the agostic bond is tilted from the aromatic plane by 11.52° , which is low compared to the 31° observed in **XIIIb**. The agostic C-H distance of 0.96 Å is very similar to that observed in **XIIIb** (0.97 Å), which is in the range of not activated aromatic C-H bonds.

The IR spectrum of **6a** is consistent with a meridional geometry of the carbonyls, giving rise to three distinct CO bands at 2043, 1958 and 1911 cm^{-1} . The significant blue-shift in the spectrum indicates a strengthening of the C-O bonds of the carbonyl ligands, owed to a reduced π -back-bonding ability of the metal, which in turn can potentially be explained by lower electron density on the metal due to π -back-bonding into the agostic C-H bond. The $^{31}\text{P}\{^1\text{H}\}$ NMR spectrum of **6a** exhibits a singlet at 53.4 ppm. Similar to **6** the carbonyl signals in the $^{13}\text{P}\{^1\text{H}\}$ NMR spectrum feature a broad singlet at 226.0 ppm and a triplet at 216.7 ppm ($J_{\text{C-P}} = 23.24\text{ Hz}$) in an integral ratio of 1:2. The *ipso*-carbon of **6a** was detected as a triplet at 84.3 ppm ($J_{\text{C-P}} = 6.63\text{ Hz}$), a significant high-field shift compared to the signal observed in **6** (cf. 173.0 ppm).

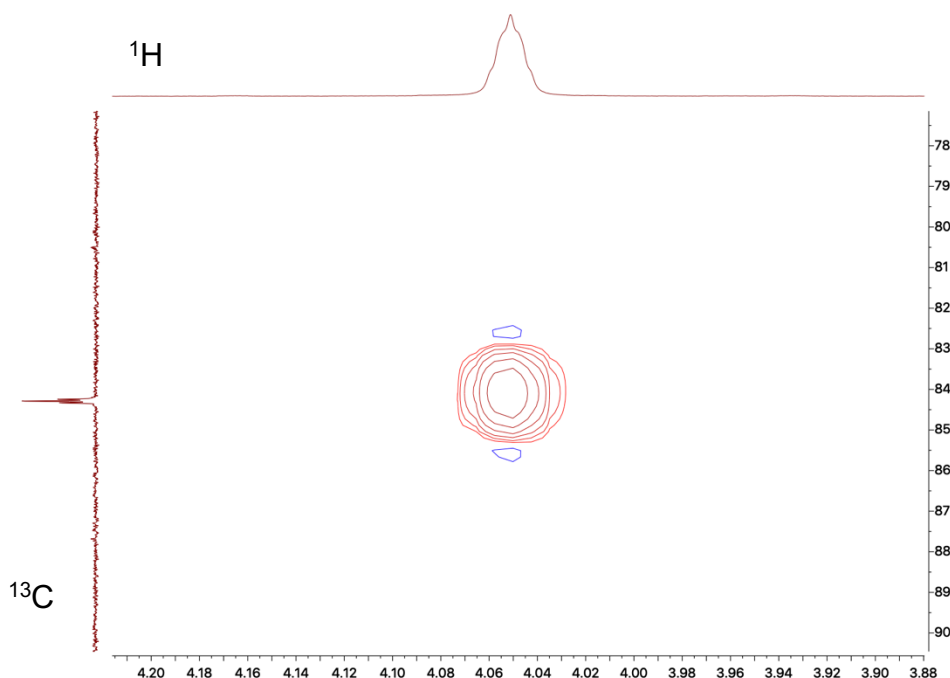


Figure 59 ^{13}C - ^1H -HSQC-spectrum in CD_2Cl_2 showing cross peak between agostic C1 and H1

Finally, by conducting a not decoupled ^{13}C experiment, a $^1J_{\text{C-H}}$ value of 139.14 Hz was measured for the agostic C-H bond, which proved to be significantly lower compared

to the values of the other two coupling constants of the aromatic C-H bonds of **6a** (162.26 Hz and 164.22 Hz respectively). This suggests a strong C-H metal interaction. Complex **6a** was also characterized by means of ESI-HRMS analysis. A peak consistent with a $[M-H]^+$ ion was found and identified.

Analogously to **XIII**, complex **6** was also treated with $\text{NO} \text{SbF}_6$ with the aim to replace one of the CO ligands with NO. After the reaction, however, a green solid was obtained that was identified as a mixture of three diamagnetic species and several strong CO absorption bands being observed in the IR spectrum. Only one small peak at 1753 cm^{-1} , assignable to NO could be discerned.

Treatment of **2** with $\text{Fe}_2(\text{CO})_9$ in acetonitrile under solvothermal conditions afforded a mixture of several diamagnetic species. By extraction with *n*-pentane a main compound with a chemical shift of 89.2 ppm could be isolated from the bulk, however, still, impurities of other species were present, preventing characterization of the compound. Hence, the solvothermal synthesis was repeated, this time using toluene as solvent, which cleanly afforded only one diamagnetic species as confirmed by use $^{31}\text{P}\{^1\text{H}\}$ NMR reaction control. However, due to the presence of paramagnetic impurities, ^1H NMR measurements only afforded spectra without signal splitting. By measuring single-crystals this problem was resolved, however, no signals for the CO ligands as well as the *ipso*-carbon were observed in the $^{13}\text{C}\{^1\text{H}\}$ spectrum. The single crystals were obtained by slow diffusion of *n*-pentane into a concentrated solution of **7** in THF.

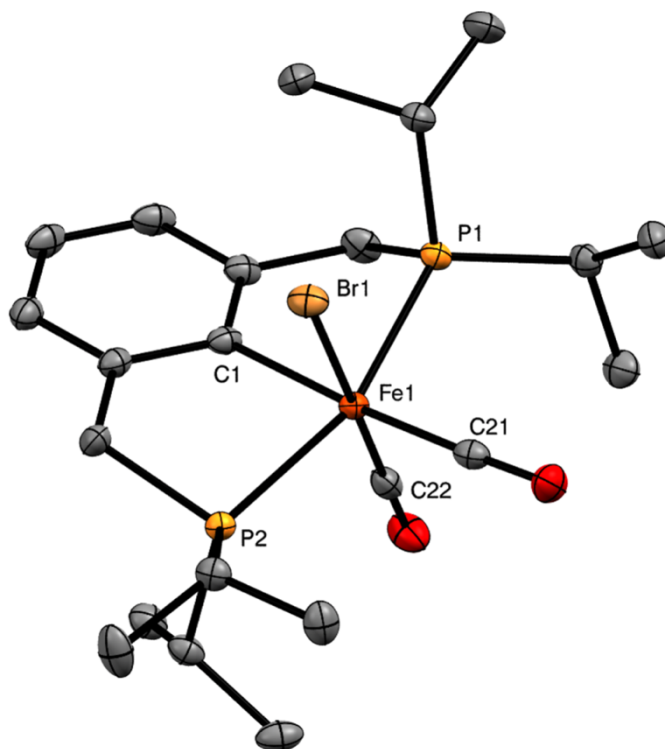


Figure 60 Crystal Structure of $[\text{Fe}(\text{PCP})(\text{CO})_2\text{Br}]$ (**7**) with 50 % thermal ellipsoids. H omitted for clarity. Selected bond lengths (Å) and bond angles (°): Fe1-C1 2.036(2), Fe1-C21 1.8050(19), Fe1-C22 1.7380(19), Fe1-Br1 2.5209(3), Fe1-P1 2.2602(5), Fe1-P2 2.2731(5), P1-Fe1-P2 160.69(2), C1-Fe1-C21 176.28(7), Br1-Fe1-C22 177.40(6).

Complex **7** features a distorted octahedral geometry. As with complexes **6** and **6a**, the phosphine-metal-phosphine bond angle shows the biggest deviation from ideality, as it was measured at 160.69° , compared to the theoretical 180° in an octahedron. The Fe1-C1 bond length is 2.036 Å, which is higher than the bond lengths observed in the phosphinite complex $[\text{Fe}(\text{POCOP})(\text{CO})_2\text{H}]$ (**XIb**) (1.995 Å) and the amine linked complex $[\text{Fe}(\text{PCP}^{\text{NEt}})(\text{CO})_2\text{Cl}]$ (**XII**) (2.002 Å), but lower than in Milstein's CH_2 -linked hydroquinone complex $[\text{Fe}(\text{PCP}^{\text{OH}})(\text{CO})_2\text{H}]$ (vide supra, Figure 31), where the bond was measured as being 2.070 Å long. The Fe1-P1 bond length is 2.260 Å, while the Fe1-P2 distance is 2.273 Å. The bond length Fe1-C21 of the basal CO ligand is with 1.805 Å longer than that of the apical carbonyl Fe1-C22 (1.738 Å).

Complex **7** shows two distinct CO bands at 1993 cm^{-1} and 1938 cm^{-1} in the attenuated total reflection infra-red (ATR-IR) spectrum, which is consistent with a complex featuring cis-carbonyl ligands. The $^{31}\text{P}\{^1\text{H}\}$ NMR spectrum of complex **7** shows as single resonance a singlet at 88.2 ppm.

A positive ion ESI-HRMS was measured of complex **7**. A peak at 449.1448 m/z assigned to the $[M-Br]^+$ ion was detected. Figure 61 shows the measured pattern on top and the simulated isotope pattern below.

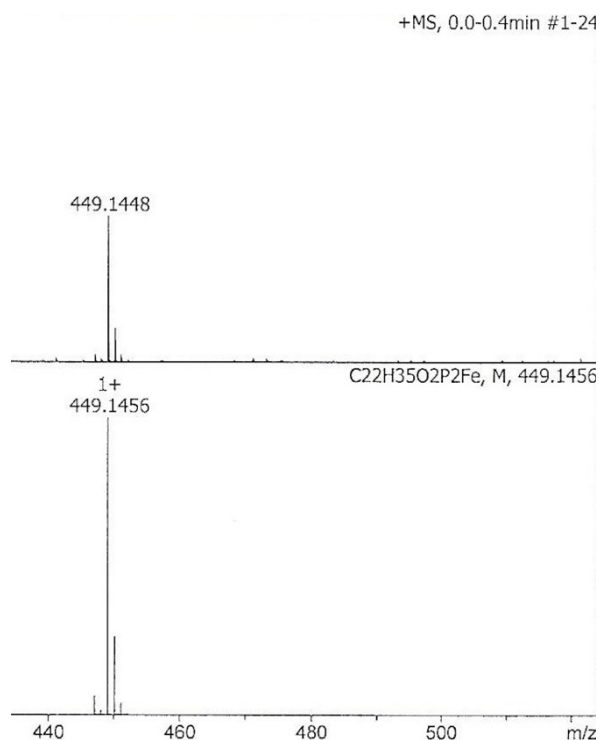


Figure 61 Positive-ion ESI full scan mass spectra of $[Fe(PCP)(CO)_2Br]$ (**7**)

In an NMR tube experiment, complex **7** was treated with $Li[HBet_3]$ leading to a rapid color change from yellow to turquoise. In the 1H NMR spectrum no hydride species could be detected and only a paramagnetic product with broad signals was detected. This suggests that, analogously to **XIIa**, a Fe(I) dicarbonyl species is formed in the reaction of **7** with $Li[HBet_3]$.

In order to perform a complete screening of the reactivity of the ligand with all commercially available base metal carbonyl precursors, a solvothermal reaction was also carried out with $Co_2(CO)_8$. The reaction was first conducted in acetonitrile, affording a clear green solution that showed only broad signals in the 1H -NMR spectrum. However, when an IR spectrum of the compound was measured, two distinct carbonyl bands were observed, that showed a distinct red-shift compared to Co(II) dicarbonyl PCP complex **VIIc** reported by Murugesan.⁸ The wavenumbers of the bands were however in good agreement with the Co(I) species **VIIe**.

Under the presumption of a disproportionation reaction, the solvothermal reaction was repeated with toluene as solvent. Hereby, after cooling to room temperature, precipitation of a green substance took place, while the supernatant solution showed a distinct yellowish-green tinge. The supernatant solution was separated from the green precipitate and after evaporation of the solvent, the green solid was extracted with benzene. The yellow extract was then fully characterized by means of NMR and IR spectroscopy and identified as $[\text{Co}(\text{PCP})(\text{CO})_2]$ (**8a**).

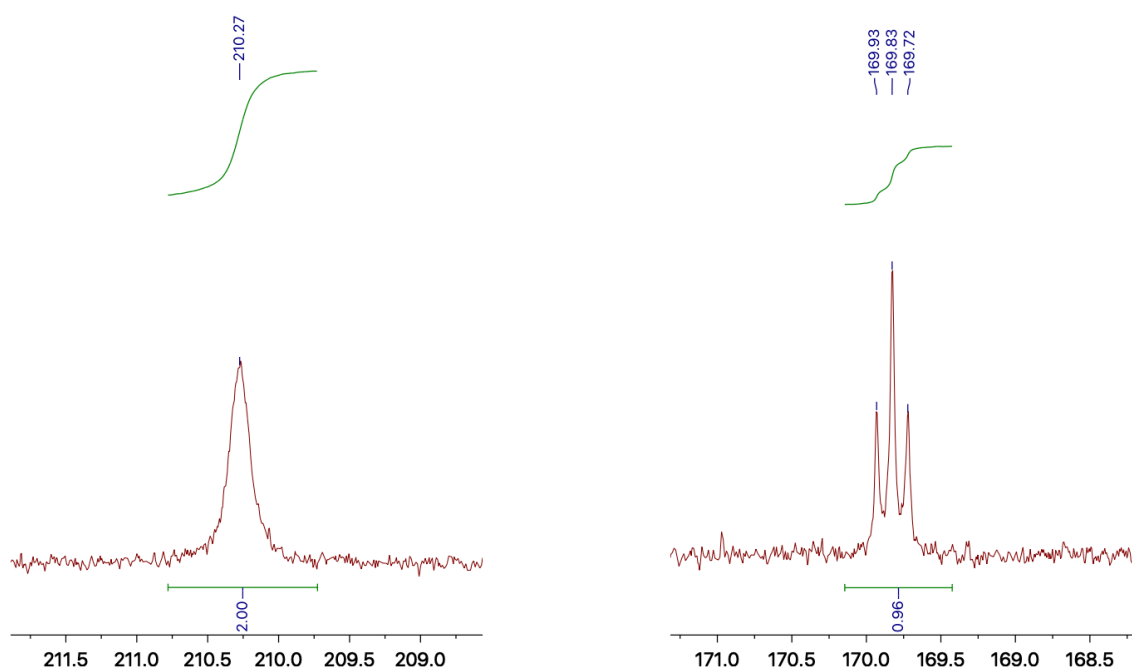


Figure 62 $^{13}\text{C}\{^1\text{H}\}$ NMR signals of the carbonyl and ipso-carbon atoms in **8a**

In the $^{31}\text{P}\{^1\text{H}\}$ NMR spectrum **8a** gives rise to a singlet at 102.9 ppm. The two carbonyl groups exhibit a broad singlet at 210.3 ppm in the $^{13}\text{C}\{^1\text{H}\}$ NMR spectrum. The ipso-carbon atom was detected as a triplet at 169.8 ppm featuring a $^1J_{\text{C-P}}$ coupling constant of 15.8 Hz. The complex features two distinct bands in the IR spectrum at 1966 cm^{-1} and 1907 cm^{-1} . The magnetic moment of the green solid **8b** was measured in solution by means of the Evans method. The calculated value of $\mu_{\text{eff}} = 3.0\ \mu_{\text{B}}$ is in good agreement with the related complex **VII d**. However, up to now, no crystals suitable for X-ray diffraction were obtained. This method is paramount to unambiguously confirm the structure of **8b**.

In inspiration of the synthesis of POCOP-Ni complexes by Zargarian, a new synthesis method for PCP-Ni complexes using only **2** and Ni powder was tested. Zargarian reported a one-pot synthesis, where, starting from resorcinol and the chlorodialkyl phosphines in presence of Ni metal -which is oxidized to NiCl₂ during the reaction-, the corresponding POCOP-Ni complexes can be obtained in good yields.⁷⁸

Similarly, it was hoped that under solvothermal conditions, with the coordinating solvent MeCN, a reactive Ni(0) species could be formed, that in turn is able to undergo oxidative addition with the ligand **2**. After stirring the reaction at 120 °C for 24 h a green solution was obtained. A ³¹P{¹H} reaction NMR showed full consumption of the ligand in the reaction mixture and a new product peak of 61.1 ppm. After evaporation of the solvent the green residue was extracted with benzene and the yellow extract was characterized using NMR spectroscopy. The ¹H, as well as the ³¹P{¹H} NMR spectrum showed that the formed product was indeed the desired Ni(II)PCP pincer complex **9**. The NMR spectroscopic data was consistent with those previously reported in literature. The complex was obtained in a yield of 75 %. The mechanism of the reaction is as of yet unknown; however, one possibility is that the reaction takes place on the metal surface itself.

4. Conclusion

In sum it was demonstrated that *ipso*-halogenated PCP pincer ligands are well equipped to function as stepping stones into the relatively unexplored field of base metal PCP pincer complexes. The ligand featured in this thesis was successfully used in oxidative addition reactions with all commercially available base metal carbonyl precursors. For many metals, the complexes reported herein are among the first known examples featuring PCP ligands, reported in literature. The ligand also was capable of undergoing oxidative addition reactions with Ni metal, constituting a novel way to synthesize these kinds of complexes. All compounds were additionally characterized using NMR, IR and ESI HRM spectroscopy as well as by means of single crystal X-ray diffraction studies.

5. References

- (1) Bullock, R. M., *Science* **2013**, 342, 1054–1055.
- (2) Mastalir, M.; Glatz, M.; Pittenauer, E.; Allmaier, G.; Kirchner, K. *J. Am. Chem. Soc.* **2016**, 138, 48, 15543–15546.
- (3) Garbe, M.; Junge, K.; Walker, S.; Wei, Z.; Jiao, H.; Spannenberg, A.; Bachmann, S.; Scalone, M.; Beller, M., *Angew. Chem., Int. Ed.* **2017**, 56, 11237-11241.
- (4) Kallmeier, F.; Kempe, R. *Angew. Chem., Int. Ed.* **2018**, 57, 46-60.
- (5) Langer, R.; Leitus, G.; Ben-David, Y; Milstein, D., *Angew. Chem., Int. Ed* **2011**, 50, 9948-9952.
- (6) Benito-Garagorri, D.; Bocokić V.; Mereiter, K.; Kirchner, K. *Organometallics* **2006**, 25, 3817-3823.
- (7) Blanksby, S. J.; Ellison, G. B. *Acc. Chem. Res.* **2003**, 36, 255-263.
- (8) Murugesan, S.; Stöger, B.; Carvalho, M.D.; Ferreira, L. P.; Pittenauer, E.; Allmaier, G.; Veiros, L. F.; Kirchner, K. *Organometallics* **2014**, 33, 6132-6140.
- (9) Murugesan, S.; Stöger, B.; Weil, M.; Veiros, L. F.; Kirchner, K., *Organometallics* **2015**, 34, 1364-1372.
- (10) Murugesan, S.; Stöger, B.; Pittenauer, E.; Allmaier, G.; Veiros, L. F.; Kirchner, K., *Angew. Chem., Int. Ed.* **2016**, 55, 3045-3048.
- (11) De Aguiar, S. R. M. M.; Stöger, B.; Pittenauer, E.; Allmaier, G.; Veiros, L. F.; Kirchner, K., *Organometallics* **2016**, 35, 3032-3039.
- (12) Tomsu, G. Neue Pyrimidin PCP Pincer Komplexe unedler Übergangsmetalle, Master Thesis, TU Wien, **2017**.
- (13) Tomsu, G.; Mastalir, M.; Pittenauer, E.; Stöger, B.; Allmaier, G.; Kirchner, K., *Organometallics* **2018**, 37, 1919-1926.
- (14) van Koten, G., *Pure Appl. Chem.* **1989**, 61, 1681-1694.
- (15) Peris, E.; Crabtree, R. H., *Chem. Soc. Rev.* **2018**, 47, 1959-1968.
- (16) Mastalir, M.; Schweinzer, C.; Weil, M.; Pittenauer, E.; Allmaier, G.; Kirchner, K., *Monatsh. Chem.* **2016**, 147, 1183-1187.
- (17) Kadassery, K. J.; MacMillan, S. N.; Lacy, D. C., *Dalton Trans.* **2018**, 47, 12652-12655.
- (18) Qi, X.; Zhao, Y.; Sun, H.; Li, X.; Fuhr, O.; Fenske, D. *New J. Chem.* **2018**, 42, 16583-16590.

- (19) Takaya, J.; Kirai, N.; Iwasawa, N. *J. Am. Chem. Soc.* **2011**, *133*, 12980-12983.
- (20) Choi, J.; MacArthur, A. H. R.; Brookhart, M.; Goldman, A. S. *Chem. Rev.* **2011**, *111*, 1761-1779.
- (21) Bernal, M. J.; Martín, M.; Sola, E., *Z. Anorg. Allg. Chem.* **2015**, *641*, 2122-2128.
- (22) Jeffrey, J. C.; Rauchfuss T. B., *Inorg. Chem.* **1979**, *18*, 2658-2666.
- (23) Garcia, P. M. P.; Ren, P.; Scopelliti, R.; Hu, X. L., *ACS Catal.* **2015**, *5*, 1164-1171.
- (24) Hasche, P.; Joksche, M.; Vlachopoulou, G.; Agarwala, H.; Spannenberg, A.; Beweries, T., *Eur. J. Inorg. Chem.* **2018**, 676-680.
- (25) Mastalir, M.; Glatz, M.; Gorgas, N; Stöger, B.; Pittenauer, E.; Allmaier, G.; Veriros, L. F.; Kirchner, K. *Chem. Eur. J* **2016**, *22*, 12316-12320.
- (26) Albrecht, M.; Kocks, B. M.; Spek, A. L.; van Koten, G., *J. Organomet. Chem.* **2001**, *624*, 271-286.
- (27) Tolman, C. A. *Chem. Rev.* **1977**, *77*, 313-348.
- (28) Moulton, C. J.; Shaw, B. L. *J. Chem. Soc., Dalton Trans.* **1976**, 1020-1024.
- (29) Gupta, M.; Hagen, C.; Flesher, R. J.; Kaska, W. C.; Jensen, C. M., *Chem. Commun* **1996**, 2083-2084.
- (30) Gauvin, R. M.; Rozenberg, H.; Shimon, L. J. W.; Milstein, D., *Organometallics* **2000**, *20*, 1719-1724.
- (31) Ohff, M.; Ohff, A.; van der Boom, M. E.; Milstein, D. *J. Am. Chem. Soc.* **1997**, *119*, 11687-11688.
- (32) Morales-Morales, D.; Redon, R.; Yung, C.; Jensen, C. M, *Chem. Commun.* **2000**, 1619-1620.
- (33) Dani, P.; Karlen, T.; Gossage, R. A.; Gladiali, S.; van Koten, G., *Angew. Chem., Int. Ed.* **2000**, *39*, 743-745.
- (34) Murugesan, S.; Kirchner, K. *Dalton Trans.* **2016**, *45*, 416-439.
- (35) Park, S., *Bull. Korean Chem. Soc.* **2001**, *22*, 1410-1412.
- (36) Schwartzburd, L.; Poverenov, E.; Shimon, L. J. W.; Milstein, D. *Organometallics* **2007**, *26*, 2931-2936.
- (37) Seul, J. M.; Park, S. *J. Chem. Soc., Dalton Trans.* **2002**, *6*, 1153-1158.
- (38) Arunachalampillai, A.; Johnson, M. T.; Wendt, O. F. *Organometallics* **2008**, *27*, 4541-4543.
- (39) Sjövall S.; Wendt, O. F., Andersson, C., *J. Chem. Soc., Dalton Trans.* **2002**, 1396-1400.

- (40) Bedford, R. B.; Draper, S. M.; Scully, P. N.; Welch, S. L. *New J. Chem.* **2000**, *24*, 745-747.
- (41) The Chemistry of Pincer Compounds, Amsterdam, Elsevier. Eds. Morales-Morales, D; Jensen, C. M. (**2007**).
- (42) Sommer, W. J.; Yu, K.; Sears, J. S.; Ji, Y.; Zheng, X.; Davis, R. J.; Sherrill, C. D.; Jones, C. W.; Weck, M. *Organometallics* **2005**, *24*, 4351-4361.
- (43) Bollinger, J. L.; Blacque, O.; Frech, C. M. *Angew. Chem. Int. Ed.* **2007**, *46*, 6514-6517.
- (44) Estudiante-Negrete, F.; Hernández-Ortega, D.; Morales-Morales, D. *Inorg. Chim. Acta* **2012**, *387*, 58-63.
- (45) Chakraborty, S.; Zhang, J.; Patel, Y. J.; Krause, J. A.; Guan, H. *Inorg. Chem.* **2013**, *52*, 37-47.
- (46) Morales-Morales, D.; Lee, D. W.; Wang, Z.; Jensen, C. M. *Organometallics* **2001**, *20*, 1144-1147.
- (47) Goldman, A. S.; Roy, A. H.; Huang, Z.; Ahuja, R.; Schinski, W.; Brookhart, M., *Science* **2006**, *312*, 257-261.
- (48) Huang, K.-W., Grills, D. C.; Han, J. H., Szalda, D. J.; Fujita, E. *Inorg. Chim. Acta* **2008**, *361*, 3327-3331.
- (49) Carrington-Smith, E. L.; Law, D. J.; Sunley, J. G.; Pringle, P. G. (BP) World Patent WO2008145976, 2008.
- (50) Timpa, S. D.; Pell, C. J.; Ozerov, O. V., *J. Am. Chem. Soc.* **2014**, *136*, 14772-14779.
- (51) Rybtchinski, B.; Vigalok, A.; Ben-David, Y.; Milstein, D., *J. Am. Chem. Soc.* **1996**, *118*, 12406-12415.
- (52) Xu, G.; Sun, H.; Li, X. *Organometallics* **2009**, *28*, 6090-6095.
- (53) Lian, Z.; Xu, G.; Li, X., *Acta Crystallogr., Sect. E.: Struct. Rep. Online* **2010**, *E66*, m636
- (54) Mastalir, M.; Tomsu, G.; Pittenauer, E.; Allmaier, G.; Kirchner, K. *Org. Lett.* **2016**, *18*, 3462-3465.
- (55) Hoskins, S. V.; Rickard, C. E. F.; Roper, W. R. *J. Chem. Soc. Commun.* **1984**, 1000-1002.
- (56) Wen, T. B.; Cheung, Y. K.; Yao, J.; Wong, W.-T.; Zhou, Z. Y.; Jia, G. *Organometallics* **2000**, *19*, 3803-3809.

- (57) Gruver, B. C.; Adams, J. J.; Arulsamy, N.; Roddick, D. M. *Organometallics* **2013**, *32*, 6468-6475.
- (58) Karlen, T.; Dani, P.; Grove, D. M.; Steenwinkel, P.; van Koten, G. *Organometallics* **1996**, *15*, 5687-5694.
- (59) Ashkenazi, N.; Vigalok, A.; Parthiban, S.; Ben-David, Y.; Shimon, L. J. W.; Martin, J. M. L.; Milstein, D. *J. Am. Chem. Soc.* **2000**, *122*, 8797-8798.
- (60) Bhattacharya, P.; Krause, J. A.; Guan, H., *Organometallics* **2011**, *30*, 4720-4729.
- (61) Jiang, S.; Quintero-Duque, S.; Roisnel, T.; Dorcet, V.; Grellier, M.; Sabo-Etienne, S.; Darcel, C.; Sortais, J.-B., *Dalton Trans.* **2016**, *45*, 11101-11108.
- (62) Dauth, A.; Gellrich, U.; Diskin-Posner, Y.; Ben-David, Y.; Milstein, D. *J. Am. Chem. Soc.* **2017**, *139*, 2799-2807.
- (63) Himmelbauer, D.; Mastalir, M.; Stöger, B.; Veiros, L. F.; Pignitter, M.; Somoza, V.; Kirchner, K. *Inorg. Chem* **2018**, *57*, 7925-7931.
- (64) Kosanovich, A. J.; Reibenspies, J. H.; Ozerov, O. V. *Organometallics* **2016**, *35*, 513-519.
- (65) Kosanovich, A. J.; Komatsu, C. H.; Bhuvanesh, N.; Pérez, L. M.; Ozerov, O. V., *Chem. Eur. J.* **2018**, *24*, 13754-13757.
- (66) Himmelbauer, D.; Stöger, B.; Veiros, L. F.; Kirchner, K. *Organometallics* **2018**, *37*, 3475-3479.
- (67) Hebden, T. J.; Schrock, R. R.; Takase, M. K.; Müller, P. *Chem. Commun.* **2012**, *48*, 1851-1853.
- (68) Himmelbauer, D.; Mastalir, M.; Stöger, B.; Veiros, L. F.; Kirchner, K., *Organometallics* **2018**, *37*, 3631-3638.
- (69) Albrecht, M.; van Koten, G., *Angew. Chem., Int. Ed.* **2001**, *40*, 3750-3781.
- (70) Rimml, H.; Venanzi, L. M. *J. Organomet. Chem.* **1983**, *259*, C6-C7.
- (71) Steenwinkel, P.; Gossage, R. A.; van Koten, G. *Chem. Eur. J.* **1998**, *4*, 759-762.
- (72) Rybtchinski, B.; Cohen, R.; Ben-David, Y.; Martin, J. M. L.; Milstein, D. *J. Am. Chem. Soc.* **2003**, *125*, 11041-11050.
- (73) Vigalok, A.; Uzan, O.; Shimon, L. J. W.; Ben-David, Y.; Milstein, D. *J. Am. Chem. Soc.* **1998**, *120*, 12539-12544.
- (74) Cherry, S. D. T.; Kaminsky, W.; Heinekey, D. M. *Organometallics* **2016**, *35*, 2165-2169.

- (75) Hebden, T. J.; St. John, A. J.; Gusev, D. G.; Kaminsky, W.; Goldberg, K. I.; Heinekey, D. M. *Angew. Chem.* **2011**, *123*, 1913-1916.
- (76) Kumar, A.; Zhou, T.; Emge, T. J.; Mirnov, O.; Saxton, R. J.; Krogh-Jespersen, K.; Goldman, A. S. *J. Am. Chem. Soc* **2015**, *137*, 9894-9911.
- (77) Rybtchinski, B.; Ben-David, Y.; Milstein, D. *Organometallics* **1997**, *16*, 3786-3793.
- (78) Vabre, B.; Lindeperg, F.; Zagarian, D. *Green Chem.* **2013**, *15*, 3188-3194.